POLITECNICO DI TORINO

Corso di laurea in Ingegneria Aerospaziale

Tesi di Laurea Magistrale

Investigation and Comparison of Hydrogen and Methane Explosive Characteristics

Relatore

Prof. Dario Pastrone

Candidato

Giuseppe Cimmino

Relatore esterno

Technische Universität München

Prof. Oskar J. Haidn

Ottobre 2018

A nonno Mario

Abstract

Hydrogen and Methane have the capability to form explosive mixtures with oxygen and air which can lead to catastrophic accidents. For this reason, explosion hazards associated with the use, storage and transport of gaseous/liquid Hydrogen and Methane are a very serious problem that does not concern only the aerospace field but, because of the increasing everyday uses of these substances, also the industrial and domestic environments. The purpose of this work is to carry out a detailed investigation on the parameters and the mechanisms governing the explosion phenomena through an accurate theoretical study and a research work on the current knowledge and data. First of all, the main features and parameters involved in hydrogen and methane combustion/oxidation processes will be discussed. Then a detailed description of chemical explosions, i.e. deflagrations and detonations, is presented. Therefore the most important differences between these two phenomena will be pointed out. Particular attention is paid to the theory of detonation waves and their main features in terms of pressure, temperature and propagation velocity. Finally a brief overwiew of some experimental tests, undertaken by NASA in order to simulate some possible launch failure scenarios involving cryogenic liquid propellants, is presented.

Contents

List of Figures

List of Tables

Nomenclature

List of Symbols

ρ	$[kg/m^3]$	Density
T	$[K]$	Temperature
c_v	$[J/(kg \cdot K)]$	Specific heat capacity at constant volume
c_p	$[J/(kg \cdot K)]$	Specific heat capacity at constant pressure
γ	$[-]$	Specific heat ratio
k	$[W/(m \cdot K)]$	Thermal conductivity
a	$[m/s]$	Speed of Sound
R^*	$[J/(kmol \cdot K)]$	Universal gas constant
R	$[J/(kg \cdot K)]$	Specific gas constant
M	$[kg/mol]$	Molar mass
p	$[atm]$	Pressure
ω	$[mol/(l \cdot s)]$	Reaction rate
q	$[J/mol]$	Heat
Φ	$[-]$	Equivalence ratio
T_{ad}	$[K]$	Adiabatic temperature
V	$[m/s]$	Velocity
h	$[J/kg]$	Specific entalpy

h_f^0	$[J/kg]$	Enthalpy of formation
h_f^s	$[J/kg]$	Sensible enthalpy
$\vec{q}$	$[J/(mol \cdot m^2)]$	Heat flux
ΔH_{f_r}	$[kJ/mol]$	Reactant heat of formation
ΔH_{f_p}	$[kJ/mol]$	Product heat of formation
ΔH_c	$[kJ/mol]$	Heat of combustion
$\underline{\underline{\tau}}$	$[N/m^2]$	Stress tensor
e	$[J/kg]$	Specific internal energy
u	$[m/s]$	Velocity along x-axis
M	$[-]$	Mach number
$1/\rho$	$[m^3/kg]$	Specific volume
S_L	$[m/s]$	Laminar burning velocity
U	$[m/s]$	Product gas velocity
S_F	$[m/s]$	Laminar flame speed
T_i	$[K]$	Ignition Temperature
δ	$[mm]$	Deflagration thickness
p_u	$[atm]$	Unburned mixture pressure
p_b	$[atm]$	Burned mixture pressure
V_{CJ}	$[m/s]$	Chapman-Jouguet velocity
U_{CJ}	$[m/s]$	Equilibrium gas velocity
λ	$[mm]$	Detonation cell width
Δh	$[J]$	Enthalpy
τ_i	$[ms]$	Induction time
E_0	$[kJ]$	Critical energy
R_s^*	$[mm]$	Detonation kernel

M_s^*	$[-]$	Critical Mach number
a_o	$[m/s]$	Unburned gas speed of sound
E_{TNT}	$[cal/g]$	TNT explosion energy
η	$[-]$	Explosion efficiency
Δ_i	$[m]$	Induction zone length
T_{VN}	$[K]$	Post-shock temperature
p_{VN}	$[atm]$	Post-shock pressure
T_{CJ}	$[K]$	Equilibrium temperature
p_{CJ}	$[atm]$	Equilibrium pressure
p_B	$[atm]$	Bubble pressure
p_{g_0}	$[atm]$	Partial gas pressure
R_0	$[mm]$	Initial bubble radius
r	$[mm]$	Liquid droplet radius
Re	$[-]$	Reynolds number
Ee	$[-]$	Weber number
μ	$[Pa \cdot s]$	Dynamic viscosity
σ	$[N/m]$	Surface tension

Abbreviations

GH2	Gaseous Hydrogen
GOX	Gaseous Oxygen
GN2	Gaseous Nitrogen
LH2	Liquid Hydrogen
LOX	Liquid Oxygen
LCH4	Liquid Methane
GCH4	Gaseous Methane
ST	Standard
STOIC	Stoichiometric
MIE	Minimum ignition energy
AIT	Auto-ignition temperature
LFL	Lower flammability limit
UFL	Upper flammability limit
MOC	Minimum oxygen concentration
CJ	Chapman-Jouguet
ZND	Ze'ldovich-Von Neuman-Doring
VN	Von-Neuman
DDT	Deflagration-to-detonation transition

Chapter 1

Introduction

The high energy density of Hydrogen ($120 \div 140$ MJ/kg) and Methane ($50 \div 55$ MJ/kg) makes them desirable and attractive as possible sources of energy. For instance, liquid hydrogen is currently the most used fuel propellant for liquid rockets in aerospace applications; on the other hand, methane is prevalently utilised in industry and domestic environments, even if many projects are under development in order to make liquid methane the main propellant of next generation rockets. Next to the obvious energy benefits, hydrogen and methane present some disadvantages related prevalenty to their explosive character. An accidental gas leak or liquid spill of these substances, infact, may generate, in combination with an oxidizer like oxygen or air, an explosive gaseous mixture which can lead to very strong explosions. To avoid and prevent these scenarios, many tests and studies have been carried out during the years in order to understand the conditions under which an explosion can occur and what are its fundamental characteristics. Therefore it appears reasonable to ask what is an explosion.

An explosion can be defined very simply as a violent and sudden release of energy; in nature it can be of different types: *chemical, physical, mechanical etc.* This work focuses on *chemical explosions*, in which the sharp energy release is due to very fast oxidation reactions between a fuel and an oxidant. Every reaction, including combustion one, takes place at a particular velocity depending on initial pressure and temperature, and it is precisely the reaction kinetics to determine the explosive behaviour of a mixture or not. So explosive mixtures are those in which reactions occur quickly. In fact, if reactions proceed slowly, the produced energy will be dissapated; instead, if they are very fast, there is no enough time for energy to be dispelled, thus a great amount of energy is deposited instaneously in a small volume causing an abrupt increase of temperature and pressure. Then the violent energy release results in the rapid expansion of the surrounding enviroment with the consequent formation of pressure waves.

Chemical explosions can be divided into *deflagrations* and *detonations*. Deflagration, also called flame, is a subsonic combustion process regulated essentially by heat conduction and radical diffusion. Through the combustion wave, oxidation mechanisms take place with the consequent transformation of reactants into products and, at the end of the process, temperature of the gases is greater whereas pressure and density decrease. Of course, a minimum energy is required to ignite the mixture and the fuel concentration must lie in specific limits (*flammability limits*) to allow the wave to propagate inside the mixture. Detonation, instead, is a supersonic process. It basically consists of a reagent shock wave: in fact, just behind the wave, temperature and pressure are such that reactions get started. Therefore a detonation scenario is much more dangerous than deflagration, because of the extremely high values of temperature and pressure that may be reached.

1.1 Thesis structure and goal

Safety and blast hazards related to the use, storage and transport of flammable substances like hydrogen and methane, both in gaseous and liquid phase, are really important issues that concern not only the aerospace but different fields. This work is therefore born with the idea of collecting and analyzing the current knowledge and data on hydrogen and methane in order to compare their explosive behaviour and features. About that, the most important combustion characteristics like oxidation mechanisms, flammability limits, auto-ignition temperature etc. for hydrogen and methane systems will be first discussed.

In Ch.3,4 a detailed study on chemical explosions (deflagrations and detonations) is presented. In particular, about denotation waves, the most important aspects and results of Chapman-Jouguet and Zel'dovich-Von Neuman-Doring theories and the different mechanism of detonation on-set are reported. Then, the outcomes from analysis on unconfined mixture detonations are ilustrated in order to point out the differences between detonation characteristics of hydrogen and methane in terms of temperature and pressure. Analysis have been conducted considering as oxidant both air and oxygen, and examining the effects of initial temperature and composition on the final equilibrium state.

In the last chapter a discussion about some experimental tests carried out by NASA on cryogenic liquid propellant, in particular HOVI test, is developed. The aim of these tests involving liquid hydrogen and liquid oxygen is to investigate and better understand their capability to self-ignite if they come into contact, for example, during some possible failure launch scenarios. Moreover, a comparison between HOVI test results and theoretical analysis on gaseous mixtures is illustrated. As this phenomenon still presents some unknowns, above all about the cause of the initial ignition, a possible cavitation-induced ignition mechanism, proposed recently to justify self-ignition of cryogenic propellant in HOVI test, is explained.

Similar tests on liquid methane have not been conducted yet, because of the still poor use of this propellant in aerospace field, therefore, no liquid methane experiments have been analyzed here. However some considerations in accordance with the information presented in this work have been made.

1.2 Fuels and Mixtures

In this work the explosive behaviour of Hydrogen and Methane will be discussed. Actually, it would be more correct to talk about fuel-mixtures because to have any explosive chemical reaction a fuel and an oxidant are necessary.
The most important physical and chemical properties, in relation to this work, of Hydrogen and Methane are reported in tab.1.1. These latter are refferred to the pure substances, so they can be quite different when a mixture is considered.

Table 1.1: Hydrogen and methane properties

Property	*Hydrogen*	*Methane*
Formula	H_2	CH_4
Molar Mass (g/mol)	2.016	16.043
Density at std cond. (kg/m^3)	0.08189	0.6517
Denisty at liquid state (kg/m^3)	70.8	422
Boiling Point (K)	20.2	111
Critical Temperature (K)	32.9	190
Gas Constant ($J/kg \cdot K$)	4125.5	518.3
Specific Heat Capacity ($J/kg \cdot K$)	14311	2229
Specific Heat Ratio γ	1.405	1.31
Thermal Conductivity ($W/m \cdot K$)	0.186	0.0360
Speed of Sound at std (m/s)	1318	450.1

At standard condition (T=298 K, p=1 atm) hydrogen and methane are in gaseous state. They can be in the liquid state at very low temperatures and for this reason in the liquid phase they are said *cryogenic*. To exist as liquids at atmospheric pressure, they have to be stored below their critical temperature which is equal to 32.9 K for hydrogen and 190 K for methane. However to have only the liquid phase with no evaporation process, hydrogen and methane must be cooled respectively below 20 K and 111 K, so their storage and trasportation is done by means of special tanks. In any case, they have to be in gaseous phase for the combustion to occur, therefore this work will focus mainly on gaseous mixture.

Properties like heat capacity, thermal conductivity and speed of sound play an important role in explosive phenomena, therefore their dependence on temperature and mixture composition will be analyzed more in detail. For their valuation, an ideal mixture of perfect gases is considered, in which the oxydant is represented by oxygen or air.

Specific Heat Capacity

The specific heat capacity of a substance or a mixture represents the amount of heat per unit of mass to provide a system for increasing its temperature by one

Kelvin degree. Depending on the type of transformation, isochoric or isobar, it can be defined a specific heat at constant volume (c_v) or at constant pressure (c_p). The ratio $\frac{c_p}{c_v}$ is called specific heat ratio or adiabatic index (γ) which is very important in isoentropic process such as the calculation of the speed of sound in a gas. Variation of these parameters is illustrated in the next figures (fig.1.1,1.2).

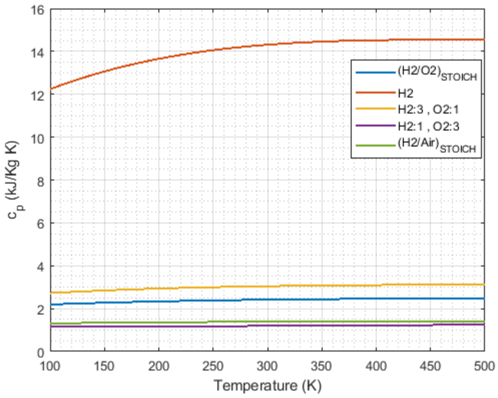

(a) c_p

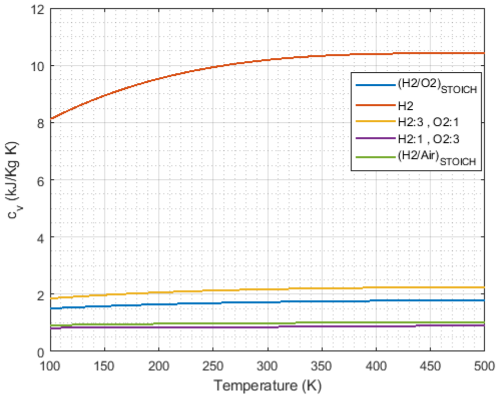

(b) c_v

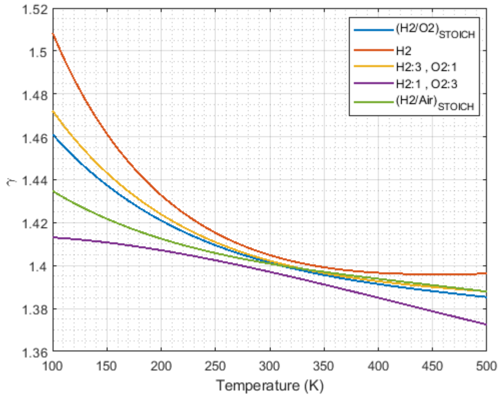

(c) γ

Figure 1.1: Hydrogen Mixtures

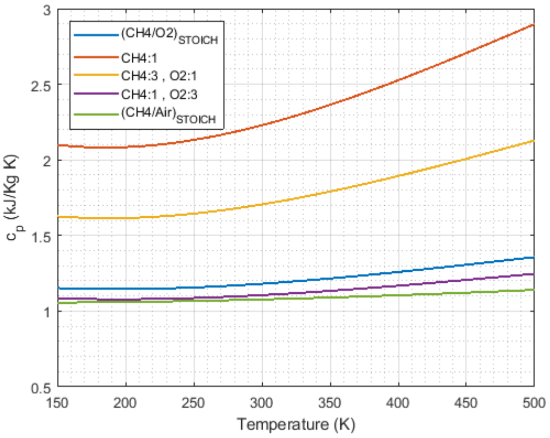

(a) c_p

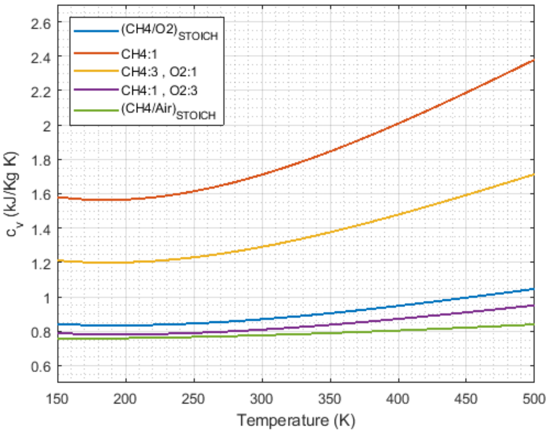

(b) c_v

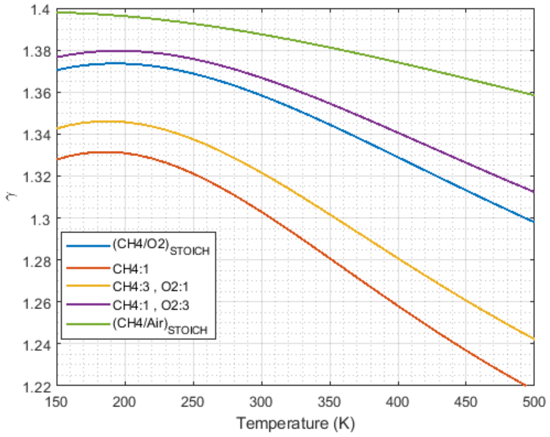

(c) γ

Figure 1.2: Methane Mixtures

Thermal Conductivity

Thermal Conductivity (k) is a measure of the ability of a substance to tranfer heat by conduction. It's equal to:

$$k = \frac{q}{\nabla T}$$

where q is the heat flux and ∇T is the temperature gradient that causes the passage of heat from the hot gas to the cold one. For example, this quantity has a key role in deflagration phenomena (see Sec.3.3.1) in which the flame propagates by heat conduction.

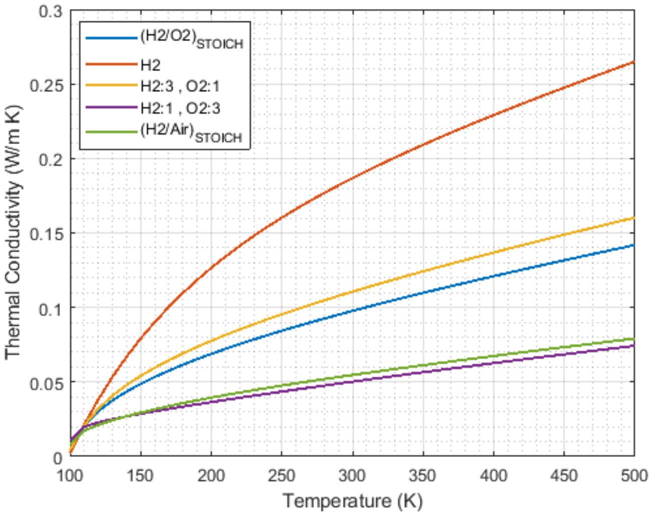

(a) *Hydrogen*

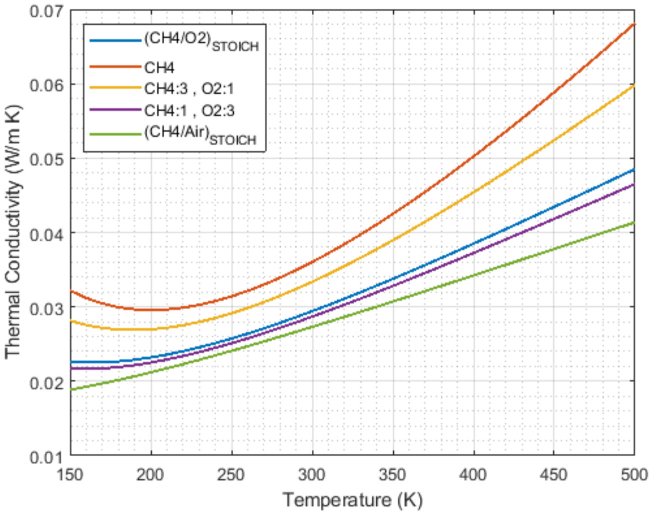

(b) *Methane*

Figure 1.3: Thermal Conductivity

Fig.1.3 shows that precence of oxygen and nitrogen decreases the capacity of the fuel to transmit heat and, moreover, at higher temperatures conduction is favorite. Anyway hydrogen mixtures present greater values of k than methane ones, so they conduct better heat. This is one of the reasons for which burning velocity is much higher in hydrogen systems (fig.3.5).

Speed of Sound

The Speed of Sound is a fundamental property of a material. It represents the velocity at which small disturbances move through a medium. In a gas, disturbance transimission is due to the the randomly collisions among the moving molecules, which is an isoentropic process. Matematically, it's equal to $a^2 = \left(\frac{\delta p}{\delta \rho}\right)_s$. After some manipulation, assuming an ideal gas, a simpler relation is obtained:

$$\boxed{a = \sqrt{\gamma \frac{R^*}{M} T}} \tag{1.1}$$

where $R^* = 8314$ J/kmol K is the universal gas constant and M is the molar mass. For an ideal mixture $M = \sum M_i x_i$ in which M_i is the molar mass of the i-th component and x_i its concentration in the mixture.

Speed of sound is strongly influenced by temperature and molar mass (fig.1.4). Increasing the temperature, molecules collisions increase too, resulting in a higher disturbance propagation speed. Furthermore, the speed of sound is lower in all the mixtures, compared to the only fuel, because of the bigger molecular weight due to the presence of oxygen and/or nitrogen. However, as hydrogen is much lighter than methane, speed of sound is greater in hydrogen mixtures.

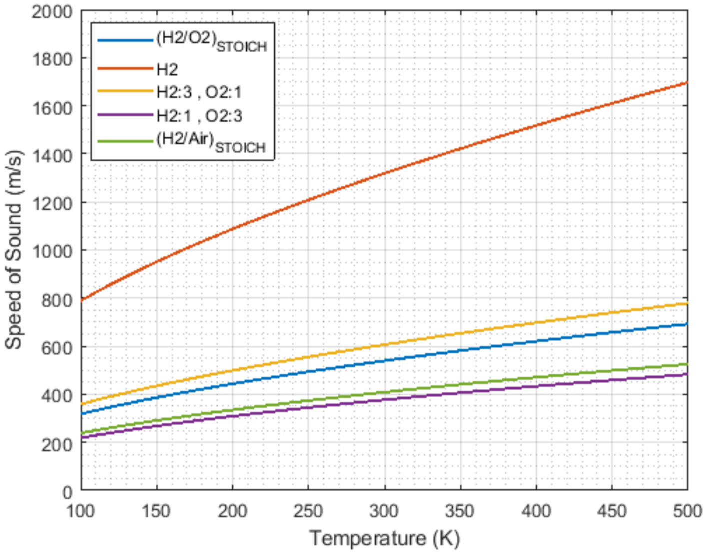

(a) *Hydrogen*

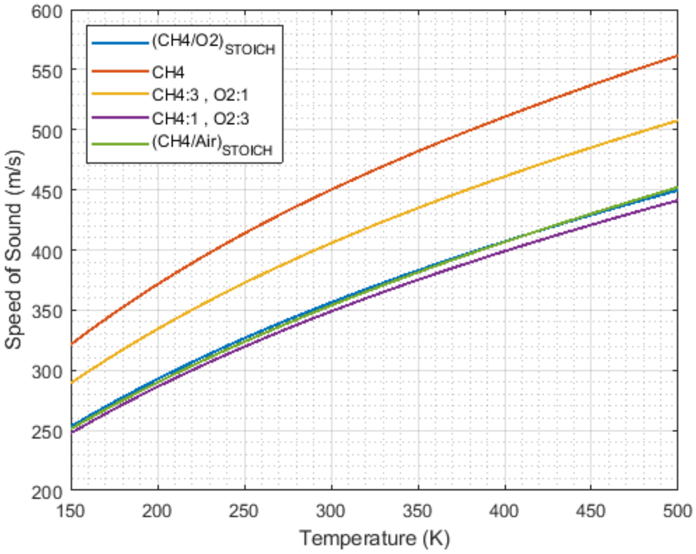

(b) *Methane*

Figure 1.4: Speed of Sound

Chapter 2

Combustion characteristics

Combustion is an exothermic chemical process between a fuel and an oxidant. It practically consists in a redox reaction in which a chemical specie (fuel) loses electrons for another (oxidant) with release of heat. At the end of combustion, the fuel and oxidant combination produces new substances called "*exhaust*" [11, 12]. For example pure water is formed by the complete combustion of hydrogen in oxygen (eq.2.1a) or air (eq.2.1b).

$$2H_2 + O_2 \rightarrow 2H_2O \tag{2.1a}$$

$$2H_2 + O_2 + 3.76N_2 \rightarrow 2H_2O + 3.76N_2 \tag{2.1b}$$

In methane combustion, a molecule of methane reacts with two oxygen ones to form water and carbon dioxide (eq.2.2a), whereas for combustion in air the nitrogen presence has to be considered (eq.2.2b).

$$CH_4 + 2O_2 \rightarrow CO_2 + 2H_2O \tag{2.2a}$$

$$CH_4 + 2O_2 + 7.52N_2 \rightarrow CO_2 + 2H_2O + 7.52N_2 \tag{2.2b}$$

Despite the preceding reactions (eq.2.1,2.2) are very simple, actually hydrogen and methane combustion is a chain reaction made up by the repeating of complicated elementary radical reactions. In a chain reaction the free radicals are continuously produced, sustained and destroyed in order to maintain the combustion.

2.1 Chemical Kinetics

A single chemical reaction can be expressed by the following complete general stochiometric relations:

$$\sum_{i=1}^{N} \nu_i^{'} M_i \longleftrightarrow \sum_{i=1}^{N} \nu_i^{''} M_i \tag{2.3}$$

where $\nu_i^{'}$ and $\nu_i^{''}$ are the stoichiometric coefficient for reagents and products, and M specifies the chemical species.

In particular, all chemical reactions, including combustion type (see later), happen at a specific rate ω depending prevalently on temperature as well as the concentration of the reactants. This reaction rate expresses how quickly or slowly the concentration of the reactants (products) varies; moreover, it is proportional to the product of the concentrations:

$$\omega = k \prod_{i=1}^{N} C_i^{\nu_i} \tag{2.4}$$

Since reactions can be forward and backward, the net reaction rate can be calculated using eq.2.4 for reagents and products:

$$\omega = k_f \prod_{i=1}^{N} C_i^{\nu_i^{'}} - k_b \prod_{i=1}^{N} C_i^{\nu_i^{''}} \tag{2.5}$$

The proportionality factor k that appears in the reaction rate relations is called "specific reaction rate". It's a function of temperature and so it provides the dependence of the reaction rate on temperature. The *"Arrhenius Law"* (eq.2.6) gives the simplest way to evaluate $k(T)$:

$$k = Ae^{-\frac{E_a}{RT}} \tag{2.6}$$

where A is the gas kinetic collision frequency or preexponential factor and the exponential term is the Boltzman factor in which E_a is the activation energy, i.e. the minimum required energy to make a reaction possible.

2.1.1 Hydrogen/Oxygen Mechanism

The H_2/O_2 oxidation is a well-known example of a chain reaction mechanism consisting of initiation, propagation and termination steps with branching. The studies

about "Explosion Limits" have played a fundamental role in hydrogen-oxygen oxidation comprehension. Here a simplified chemical reaction model, that includes the main steps, is described. For each elementary reaction, Arrhenius law can be used to evaluate the reaction rate coefficient.
Hydrogen and Oxygen combustion can be initiated by three possible reactions which have to provide radicals for the chain system:

$$H_2 + M \Leftrightarrow H + H + M \tag{2.7}$$

$$O_2 + M \Leftrightarrow O + O + M \tag{2.8}$$

$$H_2 + O_2 \Leftrightarrow HO_2 + H \tag{2.9}$$

where M can be any stable molecule.

These reactions are endothermic. The most probable initiation step is represented by (2.9) since it requires less activation energy (55 kcal/mol), while at high temperatures (2.7) and (2.8) prevail.

The production of H radicals from the previous relations initiates the chain branching mechanism, which result in an exponential growth of H, O and OH:

$$H + O_2 \Leftrightarrow O + OH \tag{2.10}$$

$$O + H_2 \Leftrightarrow H + OH \tag{2.11}$$

$$OH + H_2 \Leftrightarrow H + H_2O \tag{2.12}$$

$$O + H_2O \Leftrightarrow OH + OH \tag{2.13}$$

In the final steps, these radicals react to generate water according to the following exothermic reactions that result in chemical energy release in the form of heat:

$$H + O + M \Leftrightarrow OH + M \tag{2.14}$$

$$HO_2 + H \Leftrightarrow H_2O + OH \tag{2.15}$$

$$H + O_2 + M \Leftrightarrow HO_2 + M \tag{2.16}$$

$$OH + HO_2 \Leftrightarrow H_2O + O_2 \tag{2.17}$$

$$OH + H + M \Leftrightarrow H_2O + M \tag{2.18}$$

As pressure increases the system moves to a steady reaction condition in which the dominant chain branching step ”must be more pressure-sensitive” [23]. So, reaction (2.16) becomes more frequent than (2.10) and HO_2 production assumes an important role.

With further increase in pressure, HO_2 radical reacts with H_2 (2.19) and produces hydrogen peroxide (H_2O_2) which leads to OH active specie by (2.20); instead, (2.21)-(2.23) reactions take place at higher temperature and more radicals are produced.

$$HO_2 + H_2 \Leftrightarrow H_2O_2 + H \tag{2.19}$$

$$H_2O_2 + M \Leftrightarrow OH + OH + M \tag{2.20}$$

$$HO_2 + HO_2 \Leftrightarrow H_2O_2 + O_2 \tag{2.21}$$

$$HO_2 + H \Leftrightarrow OH + OH \tag{2.22}$$

$$HO_2 + O \Leftrightarrow OH + O_2 \tag{2.23}$$

So, below 900 K the recombination step (2.16) dominates whereas reaction (2.10) prevails for higher temperatures. In these conditions, the main termination steps are mostly recombination reactions which are strongly exothermic and release heat:

$$H + H + M \Leftrightarrow H_2 + M \tag{2.24}$$

$$O + O + M \Leftrightarrow O_2 + M \tag{2.25}$$

$$H + O + M \Leftrightarrow OH + M \tag{2.26}$$

$$H + OH + M \Leftrightarrow H_2O + M \tag{2.27}$$

Explosion Diagram

Previous reactions can be related to the explosion diagram for $H_2 - O_2$ (fig.2.1). The therm *”explosive”* is referred to very fast reactions which can lead to rapid heat releases (*explosions*). At high temperatures hydrogen-oxygen mixtures are always explosive while at low temperatures they can move from an explosive condition to a nonexplosive one and viceversa.

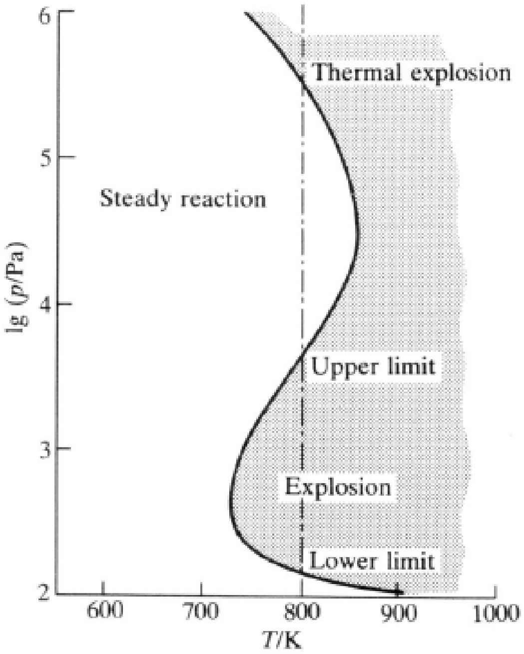

Figure 2.1: Explosive limits of hydrogen/oxygen stoichiometric mixture

The diagram is obtained by introducing a stoichiometric $H_2 - O_2$ mixture in a closed vessel. The p-T curve represents a boundary between a region of fast reactions and a region of slow reaction. Equivalently it can be interpreted as a limit for mixture auto-ignition. At low temperature and pressure, i.e. below the first explosion limit, chain branching do not occur because (2.10) can not propagate. In fact the collision and destruction of H, O, OH species by vessel walls overcomes their production and the reaction stops. Increasing the pressure, also the density increases, so the diffusion of species to walls is humpered and fast reactions occur. At high pressures, the second explosion limit is reached and three-body reactions, in which the species involved are in major concentration, become dominant (2.16). The third limit is a thermic limit due to the fact that at very high pressure the general exothermic reaction is too fast and so the heat can not be dissipated [23].

Comprehension and evaluation of this limits are very important: in fact, considering a shock wave propagating into an hydrogen-oxygen/air mixture, if the shock is strong enough, then post-shock conditions can overcome the explosion limits and reactions occur spontaneously. For example, this what happens in a C-J detonation.

2.1.2 Methane/Oxygen Mechanism

Methane/Oxygen (air) mixtures ignition is more difficult than hydrogen/oxygen (air) because C - H bond requires more energy to be broken and to allow reaction starts. There are different initiation steps depending on temperature: at low temperatures methane reacts with oxygen (2.28) while at high temperatures with radicals (2.29)-(2.31):

$$CH_4 + O_2 \Leftrightarrow CH_3 + HO_2 \tag{2.28}$$

$$CH_4 + H \Leftrightarrow CH_3 + H_2 \tag{2.29}$$

$$CH_4 + O \Leftrightarrow CH_3 + OH \tag{2.30}$$

$$CH_4 + OH \Leftrightarrow CH_3 + H_2O \tag{2.31}$$

Then, based on oxygen concentration, the following reactions can occur ((2.32) for high concentrations of oxygen and (2.33) for low concentrations):

$$CH_3 + O_2 \Leftrightarrow CH_2O + OH \tag{2.32}$$

$$CH_3 + O \Leftrightarrow CH_2O + H \tag{2.33}$$

The produced formaldehyde (CH_2O) dissociates to form CHO ((2.34)-(2.36)) radicals which combine with oxygen or other molecules M to form carbon monoxide CO ((2.37)) and (2.38)):

$$CH_2O + O_2 \Leftrightarrow CHO + HO_2 \tag{2.34}$$

$$CH_2O + HO_2 \Leftrightarrow CHO + H_2O_2 \tag{2.35}$$

$$CH_2O + CH_3 \Leftrightarrow CHO + CH_4 \tag{2.36}$$

$$CHO + O_2 \Leftrightarrow CO + HO_2 \tag{2.37}$$

$$CHO + M \Leftrightarrow CO + M + H \tag{2.38}$$

Finally, in termination steps, carbon monoxide oxides to produce carbon dioxide and energy:

$$CO + O_2 \Leftrightarrow CO_2 + O \tag{2.39}$$

$$CO + OH \Leftrightarrow CO_2 + H \tag{2.40}$$

$$CO + H_2O \Leftrightarrow CO_2 + H_2 \tag{2.41}$$

At temperature around 700 K explosive reactions can take place, therefore even in methane oxidation, explosion limits can be defined. General explosion limits for methane are illustrated in fig.2.2.

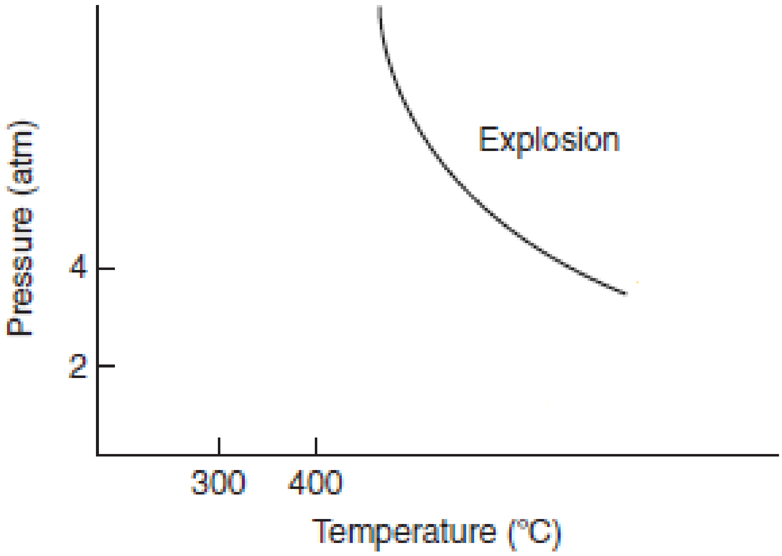

Figure 2.2: Explosive limits of methane [23]

2.2 Heat of Combustion

Heat of combustion is the quantity of heat produced during the combustion of a substance. It can be calculated as the difference between heats of formation of all products and heats of formation of all reactants (eq.2.42).

$$\Delta H_c = \sum \Delta H_{f_p} - \sum \Delta H_{f_r} \tag{2.42}$$

For hydrogen and methane complete combustion in oxygen the amount of energy released is respectively equal to -286 kJ/mol and -889 kJ/mol. The negative sign is due to the exothermic process in which the energy content of the products is lower than the energy content of the reactants, so the entalpy change is negative. The excess energy is just the energy released as heat.

2.3 Safety Characteristics

The following are the most important factors, involved in mixture combustion, which can lead or not to an explosion. Therefore they are very important in order to prevent a mixture from becoming explosive.

2.3.1 Minimum Ignition Energy

Minimum ignition energy (MIE) is defined as the minimum energy required to ignite a flammable mixture in air or in oxygen. The experimental evaluation of MIE is done by different electric sparks [20]. MIE strongly depends on fuel type, initial conditions and experimental procedure. Also the mixture composition influences the minimum ignition energy, indeed, it assumes an infinite value near the flammability limits (see later) where it is more difficult to ignite a mixture, while it is lower close to the stoichiometric condition. In particular MIE for hydrogen-air and methane-air mixtures at stoichiometric composition and 1 atm is respectively equal to 0.02 mJ and 0.3 mJ, thus hydrogen ignition requires much less energy than methane. MIE is just a concept to evaluate the tendency of a mixture to be ignite, so it is referred to the energy required to start a flame.

2.3.2 Flammability Limits

For a mixture at given pressure and temperature it is possible to define the minimum and maximum fuel concentration that allow the flame to propagate: these two limits are called ”Lower (lean) and Upper (rich) flammability limits” (LFL, UFL) or sometimes wrongly ”Lower and Upper explosion limits (LEL, UEL)”.

When the fuel concentration is very small, thus below the LFL, even if the mixture reacts, the amount of energy released is so small that temperature rise is negligible and so chemical reactions can not be sustained. Same situation occurs if the mixture is fuel-rich with a fuel concentration above the UFL. Outside the range of flammability, energy is so small that enough chain branching are not formed and chain termination takes place.

As a mixture can be ignited or a flame can propagate only within the limits, they represents a useful safety parameter. Indeed, an explosive reaction can be stopped by handling the fuel concentration in the mixture.

Here is reported a table, taken from the book ”Combustion” and from a NASA Report ([23, 10]), that compares the flammability limits for hydrogen and methane mixtures.

Table 2.1: Comparison of Flammability Limits in Oxygen and Air ([23, 10])

Fuel	O_2		Air	
	Lean	Rich	Lean	Rich
H_2(%)	5	95	5	75
CH_4(%)	5	61	5	15

The flammability interval is always greater in oxygen than in air, because nitrogen does not partecipate to the reaction but it acts as an inert.

Previous limits are evaluated at initial standard conidition. Actually flammability limits depend on initial temperature and pressure. For instance, if the initial temperature is greater than 300 K, the entalphy of the gases is higher and flammability range becomes larger.

At different temperatures, flammability limits can be evaluated through the next empirical formulas:

$$LFL_T = LFL_{T_{st}} - 0.75 \cdot \frac{T - T_{st}}{\Delta H_C} \tag{2.43a}$$

$$UFL_T = UFL_{T_{st}} + 0.75 \cdot \frac{T - T_{st}}{\Delta H_C} \tag{2.43b}$$

Eq.2.43 show that when temperature is higher than 25^oC LFL dicreases and UFL increases, whereas the opposite happens for temperatures less than standard.

The graphic representation of eq.2.43 is illustrated in fig.2.3.

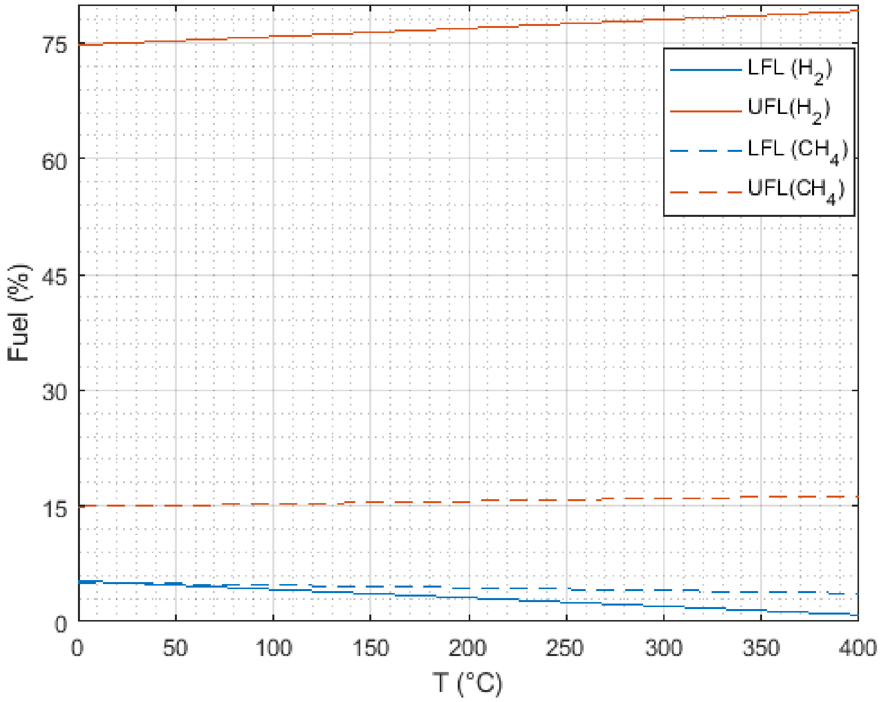

Figure 2.3: Flammability limits dependence on temperature

While the lower flammability limits is little influenced by pressure, the upper flammability limit strongly depends on pressure and, in particular, the greater is the pressure the greater is the limit (eq.2.44).

$$UFL_p = UFL_{p_{st}} + 20.6 \cdot (\log p + 1) \tag{2.44}$$

2.3.3 Minimum Oxygen Concentration

The Minimum Oxygen Concentration (MOC) is the minimum O_2 concentration in a mixture of fuel, air and inert gas below which combustion is not possible whatever the fuel concentration is [58]. This is an important safety parameter because fire or explosion can be avoided by reducing the oxygen concentration with the addition of an inert gas.

If the inert gas is nitrogen, the MOC is equal to 5% for hydrogen and 12% for methane mixtures. Knowing LFL, UFL and MOC it is possible to represent all the flammability region in a graph called ”Flammability diagram”, in which concentration of fuel, oxygen and inert gas are represented on the three axes. Air line represents all possibile combinations of fuel-air mixtures while stoichiometric line all stoichiometric fuel-oxygen mixtures. For example, a representation of the flammability diagram for methane is provided in fig.2.4.

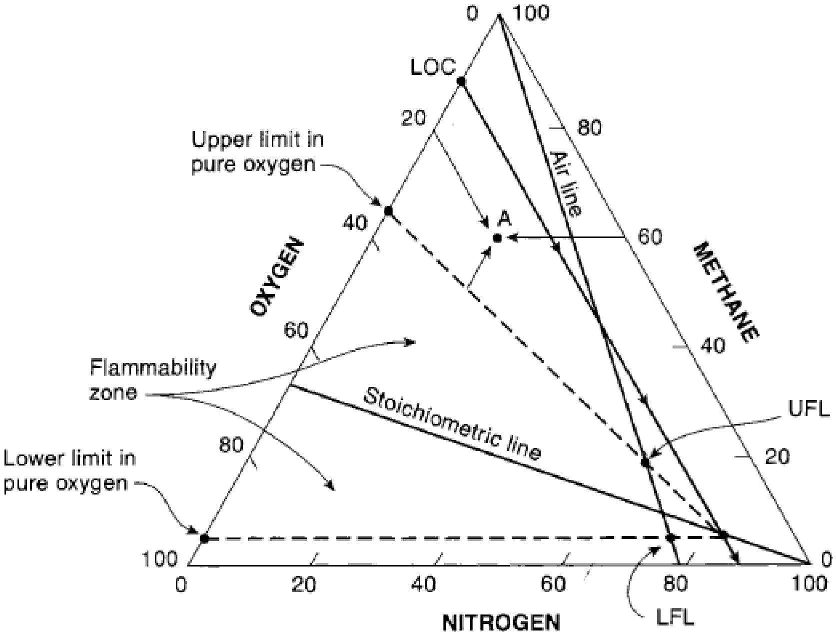

Figure 2.4: Methane flammability diagram [13]

The diagram illustrated in fig.2.4 is valid at standard conditions. Clearly the different paramenters change with pressure, temperature, fuel and inert type.

2.3.4 Auto-ignition Temperature

Very often the ignition of a fuel-oxidant mixture can occur without external source. This particular combustion type is used to be called *Auto-ignition* or *Spontaneous ignition*. Autoignition strongly depends on internal reactions, and it happens when initially slow reactions have enough branching to increase free radicals concentrations and accelerate the oxidation. These reactions heat up the mixture, so the temperature increases and ignition of the mixture takes place. The auto-ignition limits are the same showed in the explosive diagrams of fig.2.1-2.2. The initiation chain reactions in auto-ignition are quite slow, whereby a certain time is necessary for reactions to accelerate: it's called *induction time* and it represents the time required to observe ignition. According to Shepard's definition, ignition occurs at the end of an induction zone where the temperature gradient is maximum as well as the heat release [50].

Table 2.2: Autoignition Temperature (^oC) of hydrogen and methane from Kuchta (1985) [34]

Fuel	Oxygen	Air
H_2	~ 400	520
CH_4	500	630

The (minimum) autoignition temperature (AIT) is defined as the lowest temperature at which reactions start spontaneously, so AIT has the same role of an external source, i.e. it has to supply the required energy to start reactions. AIT is a function of pressure and composition.

Tab.2.2 reports AITs at atmospheric pressure and stoichiometric composition. In absence of nitrogen initiation reaction are faster and so AITs of fuel-oxygen mixtures are lower. Furthermore, methane has upper values of AITs compared to hydrogen because it requires more energy to be ignited.

2.4 Adiabatic Flame Temperature

At the end of combustion, the hot gases formed by the oxidation of the reactants can reach very high temperatures. In particular, for an adiabatic process that occurs with no work, heat or energy loss, the final temperature of the exhausted gas is called "*Adiabatic Flame Temperature*". The maximum adiabatic flame temperature for given species happens when fuel and oxidant are in "stoichiometric" composition (see fig.(2.5)), i.e. all fuel and oxidant turn into products and the combustion is said "complete" [1].

Fig.2.5 illustrates the adiabatic flame temperature behaviour for hydrogen/oxygen, hydrogen/air, methane/oxygen and methane/air mixtures with an initial temperature and pressure respectevely equal to $T_{in} = 300$ K and $p_{in} = 1$ atm for different compositions.

Φ is the equivalence ratio. It's a parameter used to estimate how much a mixture is far from the stoichiometric composition.

$$\Phi = \frac{n_{fuel}/n_{ox}}{\left(n_{fuel}/n_{ox}\right)_{st}}$$

where n is the number of moles and "*st*" stands for *stoichiometric*.

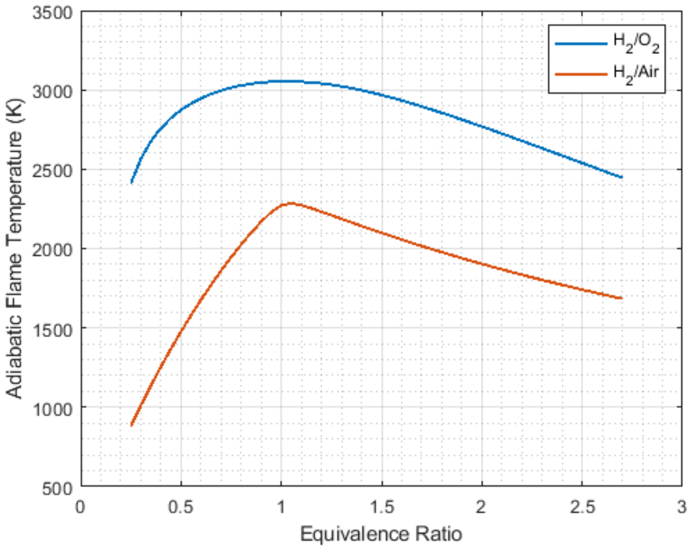

(a) *Hydrogen*

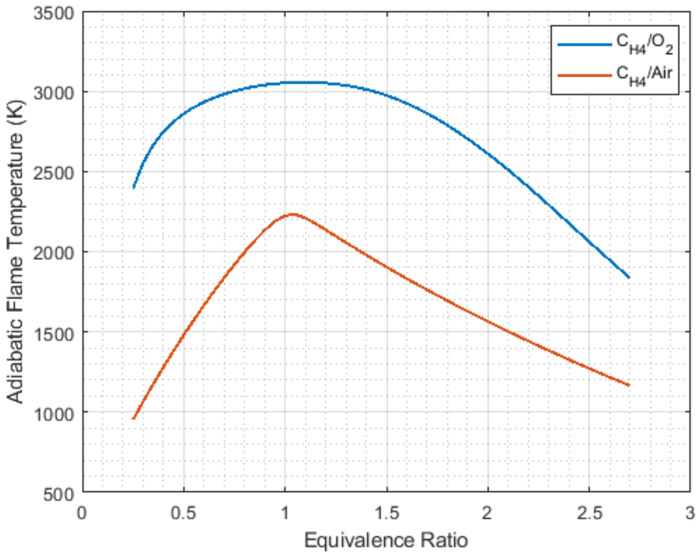

(b) *Methane*

Figure 2.5: Adiabatic Flame Temperature vs Equivalence Ratio (Φ)

Diagrams of fig.2.5 practically represent the solution of a chemical equilibrium problem and they are obtained with a specific equilibrium code [24, 32]. The maximum adiabatic flame temperature results for the stoichiometric composition ($\Phi \approx 1$). For fuel-rich system ($\Phi > 1$), the amount of oxygen is not sufficient to burn all the fuel and so the released energy is less as well as the products temperature; on the other hand, for fuel-lean system ($\Phi < 1$) heat is also transferred to the excess oxygen and even in this case the final temperature is less than stoichiometric case. In addition, the adiabatic temperature of a combustion in pure oxygen is greater in comparison to the case of combustion in air since nitrogen is present as diluent, therefore it does not partecipate to the oxidantion.

Chapter 3

Propagation Phenomena

In the previous chapter the main characteristics and parameters involved in a combustion mechanism have been analysed. The most important difference between a combustion or a fire and an explosion is the way in which energy is released. The term explosion is related to a rapid and sudden release of energy resulting in a violent expansion of the gases. These push away the sorrounding gas and initiate a pressure wave, called *blast wave*, which quickly goes away from the blast source [13].

There are several kind of explosions: in this work *chemical explosion* will be described. They are related to the sudden release of chemichal energy produced through chemical reactions which propagate within the mixture. As said before, when reaction is initiated by an ignition source, a combustion wave can propagate through the mixture if the composition lies in specific limits. Combustion waves are responsible for important thermodynamic and chemical changes which make the conversion of reagents into products possible and permit the self-sustained propagation of the combustion wave [36].

In particular, a chemical explosions can be a *Deflagration* or a *Detonation.* In a deflagration a layer of hot material heats by conduction an adjacent cold layer causing it ignition. Since the energy transfer mechanisms is slow, the combustion wave is formed by a reaction front, moving at subsonic speed, and a pressure front which gradually gets away as it propagates at a higher velocity equal to the speed of sound in the unburned mixture.

On the other hand, a detonation is a supersonic wave that propagates through shock waves. The strong compression leads the mixture above its autoignition temperature resulting in explosive reactions, and the consequent energy release supports the wave propagation [23]. In this case reaction front and shock wave are coupled.

Fig.3.1 from "Chemical Process Safety" and tab.3.1 give information about the principal differences between deflagrations and detonations.

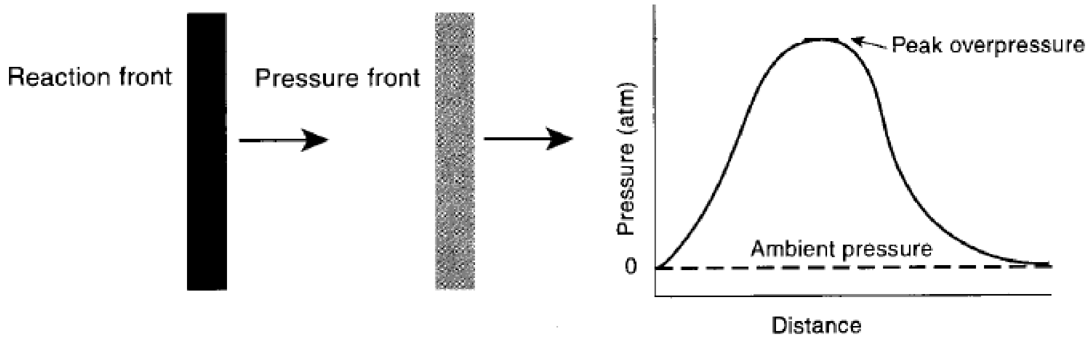

(a) *Deflagration*

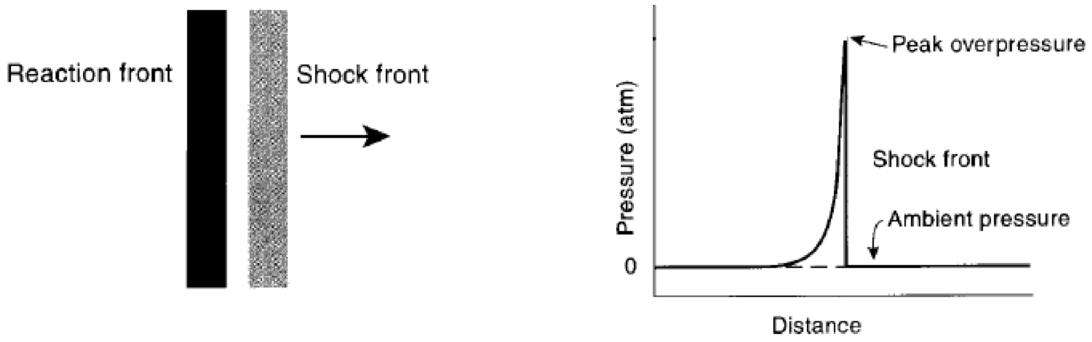

(b) *Detonation*

Figure 3.1: Propagation front

Table 3.1: Differences between deflagrations and detonations

Deflagration	**Detonation**
Subsonic propagation	Supersonic propagation
Reaction front and pressure front decoupled	Reaction front and pressure front coupled
Temperature increase	Temperature increase (greater)
Slightly pressure decrease	Pressure increase
Density decrease	Density increase

3.1 Analytical Formulation

To study the dynamics and thermodynamics of a chemically reacting flow some equations have to be introduced.

3.1.1 Governing equation

Eq. 3.1, 3.2, 3.3 represent the *"Navier-Stokes equations"*, i.e. the conservation equations of mass, momentum and energy respectively. The last equation (eq. 3.4), instead, is the specie conservation equation.

$$\frac{\partial \rho}{\partial t} + \nabla \cdot (\rho \vec{V}) = 0 \tag{3.1}$$

$$\rho \frac{\partial \vec{V}}{\partial t} = -\rho(\nabla \cdot \vec{V}) + \nabla \cdot \underline{\underline{\tau}} \tag{3.2}$$

$$\rho \frac{\partial}{\partial t}\left(h - p/\rho\right) = -\rho \vec{V} \cdot \nabla(h - p/\rho) - \nabla \cdot \vec{q} - \underline{\underline{\tau}} : (\nabla \cdot \vec{V}) \tag{3.3}$$

$$\rho \frac{\partial Y_i}{\partial t} + \nabla \cdot (\rho \vec{V} Y_i) + \nabla \cdot (\rho Y_i \vec{V_i}) = \omega_i \tag{3.4}$$

in which $\rho, p, \vec{V}$ and h are density, pressure, velocity and specific entalpy of the fluid. $\underline{\underline{\tau}}$ is the stress tensor and $\vec{q}$ is the heat flux vector. In the species equation Y_i is the mass fraction of the i-th component and $\vec{V_i}$ its diffusion velocity; ω_i is the rate of concentration change of the i-th species so it represents the reaction velocity [35]. Assuming a steady, compressible, inviscid and one dimensional flow the previous equations are simplified. In this case there is not time dependence anymore, the viscous terms disappear, the velocity has only one component in x-direction and the variations of the different quantities just occur along the x-spatial coordinate.

$$\frac{d}{dx}\Big(\rho u\Big) = 0 \tag{3.5}$$

$$\frac{d}{dx}\Big(p + \rho u^2\Big) = 0 \tag{3.6}$$

$$\frac{d}{dx}\Big(h + \frac{u^2}{2}\Big) = 0 \tag{3.7}$$

$$\rho u \frac{dY_i}{dx} = \omega_i \tag{3.8}$$

3.1.2 Auxiliary Relations

To close the differential equation system 3.1-3.4 some auxiliary relations are necessary.

Ideal Gas Equation of State:

$$p = \rho R T \tag{3.9}$$

Energy-Entalpy Relation:

$$h = \sum_{i=1}^{N} Y_i h_i = e + p/\rho \tag{3.10}$$

where N is the total number of species presented in the mixture.

Caloric Equation of State

$$h_i = h^0_{f,i} + h^s_i = h^0_{f,i} + \int_{T_0}^{T} c_{p,i} dT \tag{3.11}$$

where $h^0_{f,i}$ is the enthalpy of formation, that is the variation of enthalpy associated with the formation of the species i; h^s_i is the sensible enthalpy which represents the thermal energy content of the substance i and $c_{p,i}$ is the specific heat at constant pressure.

3.2 One-dimensional formulation

To develop a first general analysis about the variation of the different properties across a propagating wave (deflagration or detonation), a simple one-dimensional model is presented.

Consider a steady, 1D planar wave moving in a mixture with a certain velocity. In a coordinate system integral with the wave, the unburned gas moves towards the wave with velocity u_1 while the wave appears fixed (fig.3.2).

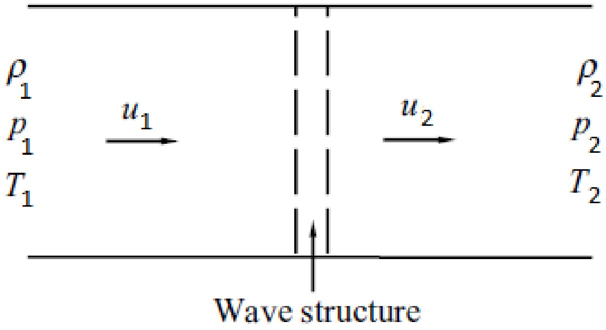

Figure 3.2: Schema of one-dimensional wave [8]

The burned gas properties downstream the wave can be calculated using the Conservation Equation (eq.3.1, 3.2, 3.3). Under the assumptions of stationarity, unidimensionality and uniaxiality, the equation system becomes the following:

$$\rho_1 u_1 = \rho_2 u_2 \tag{3.12}$$

$$p_1 + \rho_1 u_1^2 = p_2 + \rho_2 u_2^2 \tag{3.13}$$

$$c_p T_1 + \frac{1}{2} u_1^2 + q = c_p T_2 + \frac{1}{2} u_2^2 \tag{3.14}$$

$$p_{1,2} = \rho_{1,2} R T_{1,2} \tag{3.15}$$

The ideal gas equation is used to close the system. The subscripts 1 and 2 are referred respectevely to the unburned and burned condition. ”q” is the heat release due to chemical reactions, so $q = 0$ means that the system is adiabatic and no reactions occur.

3.2.1 Rayleigh Equation

Obtaining u_2 from Eq.3.12 and sobstituing in Eq.3.13:

$$\rho_1 u_1^2 - \left(\frac{\rho_1^2}{\rho_2} u_1^2\right) = p_2 - p_1$$

Dividing by ρ_1^2:

$$\boxed{u_1^2 = \frac{1}{\rho_1^2}\left[(p_2 - p_1)/\left(\frac{1}{\rho_1} - \frac{1}{\rho_2}\right)\right]} \tag{3.16}$$

Eq.3.16 is the Rayleigh relation. Since the quantity $u_1^2\rho_1^2$ is always positive, pressure and specific volume variations are of the same sign, so it follows that if $P_2 > P_1$ then $\rho_2 > \rho_1$ and viceversa.

An other form of the Rayleigh equation is obtained using the speed of sound expression and introducing the Mach number:

$$\gamma M_1^2 = \frac{\left(\frac{P_2}{P_1} - 1\right)}{\left[1 - \frac{1/\rho_2}{1/\rho_1}\right]} \tag{3.17}$$

3.2.2 Rankine-Hugoniot Equation

Sobstituing the Rayleigh Equation (eq.3.16) into Mass Conservation Equation (eq.3.12):

$$u_2^2 = \frac{1}{\rho_2^2}\left[(P_2 - P_1)/\left(\frac{1}{\rho_1} - \frac{1}{\rho_2}\right)\right] \tag{3.18}$$

Assuming that c_p and γ are constant, and considering that:

$$c_p = R\left(\frac{\gamma}{\gamma - 1}\right) \qquad RT = P/\rho \tag{3.19}$$

The Energy Equation becomes:

$$\frac{\gamma}{\gamma - 1}\left(\frac{P_2}{\rho_2} - \frac{P_1}{\rho_1}\right) - \frac{1}{2}(u_1^2 - u_2^2) = q \tag{3.20}$$

The quantity $(u_1^2 - u_2^2)$ can be evaluated subtracting term to term Eqs.(3.16) and (3.18):

$$u_1^2 - u_2^2 = \left(\frac{1}{\rho_1} + \frac{1}{\rho_2}\right)(P_2 - P_1) \tag{3.21}$$

Finally the Rankine-Hugoniot Equation is obtained from Eqs.(3.20) and (3.21):

$$\boxed{\frac{\gamma}{\gamma - 1}\left(\frac{P_2}{\rho_2} - \frac{P_1}{\rho_1}\right) - \frac{1}{2}(P_2 - P_1)\left(\frac{1}{\rho_1} + \frac{1}{\rho_2}\right) = q} \tag{3.22}$$

The Rankine-Hugoniot Equation provides all the possible solution $(1/\rho_2, P_2)$ given an initial condition $(1/\rho_1, P_1)$ and a given q (fig.(3.3)). For q=0, the classical Rankine-Hugoniot equation for non reagent shocks passing for the initial condition point is obtained.

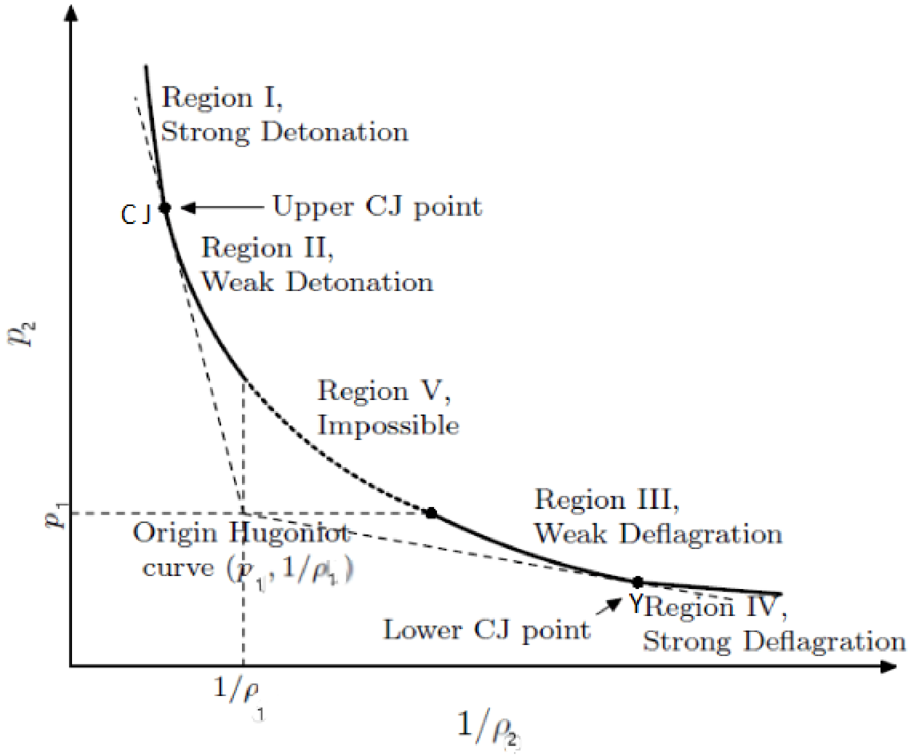

Figure 3.3: Hugoniot Curve [41]

Thanks to Rankine-Hugoniot relation it's possibile to evaluate the conditions of the burned gases downstream the wave. Thus, whatever is the burned gas state after the wave, it must lie on the Hugoniot curve for that particular initial conditions.

In fig.(3.3) the continous line curve is the Hugoniot curve for given initial conditions whereas the horizontal and vertical dashed lines represent the constant pressure and specific volume conditions and they divide the Hugoniot Curve in three regions (I-II, III-IV, V).

In I-II area, $P_2 > P_1$ and $1/\rho_2 < 1/\rho_1$, so from eq.3.17 the Mach number is positive and grater than 1. This region defines the compression or detonation solution.

In III-IV area, $P_2 < P_1$ and $1/\rho_2 > 1/\rho_1$. Overall the Mach number is positive and less than 1, so in this region the solutions are expansion or deflagration waves.

In the V region Mach number is negative, so this area does not represent any accetable physical solution.

The particular point on Hugoniot curve representing the final condition is found using Rayleigh line for a specific initial velocity. In particular, Rayleigh lines tangent to the curve are referred to the minimum detonation velocity (Upper C-J point) and the maximum deflagration velocity (Lower C-J point).

Finally, the different Propagation Phenomena represented on Hugoniot plot (fig.3.3) can be classified in this way:

- **Strong Detonation**

  $$P_2 > P_{CJ}\,(supersonic\,flow\,to\,subsonic) \quad \textbf{Region I}$$

- **C-J Detonation**

  $$P_2 = P_{CJ}\,(supersonic\,flow\,to\,sonic) \quad \textbf{Point CJ}$$

- **Strong Detonation**

  $$P_2 < P_{CJ}(supersonic\,flow\,to\,supersonic) \quad \textbf{Region II}$$

- **Weak Deflagration**

  $$P_2 > P_Y(subsonic\,flow\,to\,subsonic) \quad \textbf{Region III}$$

- **Strong Deflagration**

$$P_2 < P_Y (subsonic\, flow\, to\, supersonic) \qquad \textbf{Region IV}$$

3.3 Deflagration

As seen in the previous paragraph, "*Deflagration*" represents a subsonic combustion process in which a reagent mixture undergoes an expansion (decrease of pressure), a decrease of density and for eq.3.12 an increase of velocity, therefore it represents an expansion wave. The Rayleigh line tangent to curve in the deflagration zone identifies the Lower C-J point and it divides this region in Weak and Strong Deflagration Zone. Actually, a strong deflagration does not exist because the velocity of the products behind the flame would be higher than the sound speed; instead, in a weak deflagration the pressure reduction is negligible so the entire process can be considered almost isobaric (see Sec.3.3.2). From a macroscopic point of view, flame propagation is regulated by conduction mechanism while at microscopic level it is essentially due to molecular transport of energy and free radicals from the reaction zone to unreacted flow [48].

3.3.1 Laminar Flame Structure and Laminar Flame Speed

The region of space in which a deflagration occurs is usually defined as "*flame front*" and the spatial distribution of the thermal, fluid and chemical field as "*flame structure*" [8]. For instance, the temperature profile through a premixed flame is represented in fig.3.4.

According to Mallard and Le Chatelier theory, the flame front can be splitted out into a preheat zone and a reaction zone. The unburned mixture is first preheated by conduction from the reaction zone and so temperature increases up to the achievement of the ignition condition. Therefore in the reaction zone, chemical reactions take place and heat released is transferred to the pre-heat zone and so on. It's evident that the transferred energy must be sufficient to raise the unburned gas temperature from their initial value to their ignition temperature. Once cold gas has been heated to the autoignition temperature, there is a spurt in chemical reactions and temperature rises until its maximum value. In reality the propagation is not controlled only by heat but also by the diffusion of radicals and other species formed in the reaction zone [55, 39].

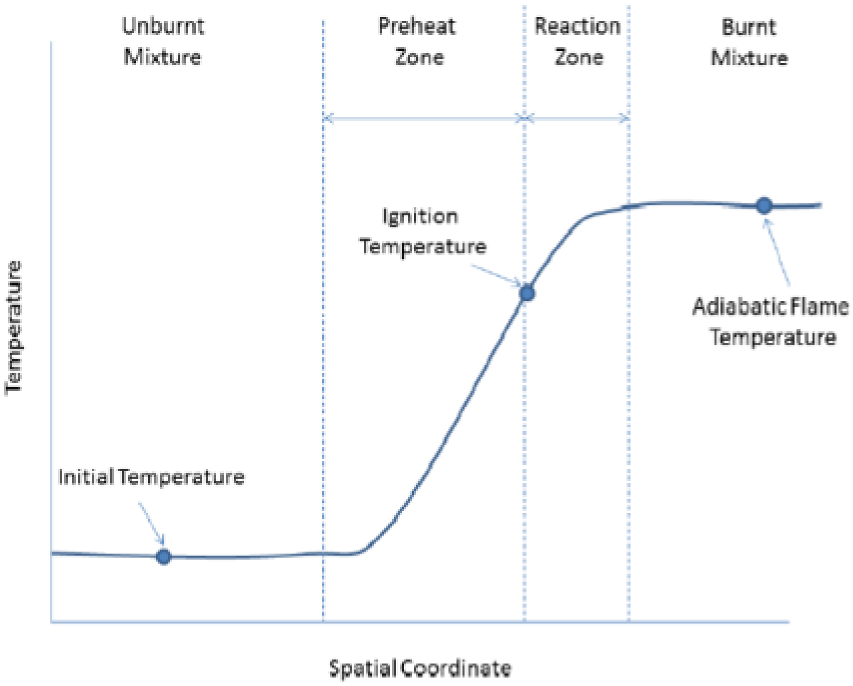

Figure 3.4: Temperature Evolution in a laminar flame wave

The *burning velocity* S is the rate at which a deflagration wave propagates relative to the unburned gas ahead of the front. The laminar burning velocity S_L is the lowest velocity that the flame would have if the system was adiabatic and there was no heat loss. On the other hand, the *flame speed* S_F is relative to a fixed observer. It can be expressed as the sum of the (laminar) burning velocity and the component U of the product gases velocity. Alternatively, it is equal to the product of the burning velocity and the *expansion ratio* E due to the decrease in density of the products after the passage of the flame [34].

$$S_F = S + U$$

$$S_F = S \cdot E$$

The (laminar) burning velocity is a property of the mixture, so it strongly depends on the composition and thermodynamic conditions of the gases. More in detail, it is connected to the thermal diffusivity $\alpha = \frac{k}{\rho c_p}$ where k is the thermal conductivity, chemical reaction rate and heat of combustion.

Consider the schema of fig.3.2. To evaluate the laminar burning velocity of a propagating flame, first it is necessary to write a heat balance equation between the pre-heat zone and the reaction zone.

$$\rho_1 S_L c_p (T_i - T_0) = k \frac{T_f - T_i}{\delta} \tag{3.23}$$

where T_0, T_i, T_f are the initial, ignition and final temperature, $\rho_1 S_L$ represents the total mass rate for unit of area entering into the deflagration wave, k is the thermal conductivity and δ is the flame thickness (i.e. the thickness of the reaction zone).

In practice, eq.3.23 states that the heat transferred from the reaction zone to the pre-heat zone is equal to the heat required to increase the temperature of the unburned gases from T_0 to ignition temperature T_i. For the conducted heat at the second member of eq.3.23 it has been supposed that the increase in temperaure is linear.

The amount of heat generated in the reaction zone is also equal to the product among the chemichal reaction rate ω, the volume (which in 1D approximation becomes δ) and the heat generated per mole q. Again this heat increases the temperature of the mass flow gases to T_i:

$$\omega \delta q = \rho_1 S_L c_p (T_i - T_0) \tag{3.24}$$

Substituting eq.3.24 into eq.3.23 and solving in S_L, the final expression for the laminar burning velocity, at which the flame propagates in the unburned mixture, is obtained (eq.3.25):

$$\boxed{S_L = \frac{1}{\rho_1 c_p} \sqrt{\frac{k \omega q}{T_i - T_0}}} \tag{3.25}$$

Eq.3.25 shows that deflagration propagation velocity strongly depends on density: velocity increases as density decreseas, hence in hydrogen mixtures laminar burning is much greater than methane ones.

The approximate trend of hydrogen and methane burning velocity with mixture composition is shown in fig.3.5. The values used in the evaluation are taken from *"Effect of molecular structure on burning velocity"* of Gibbs and Calcolate [22].

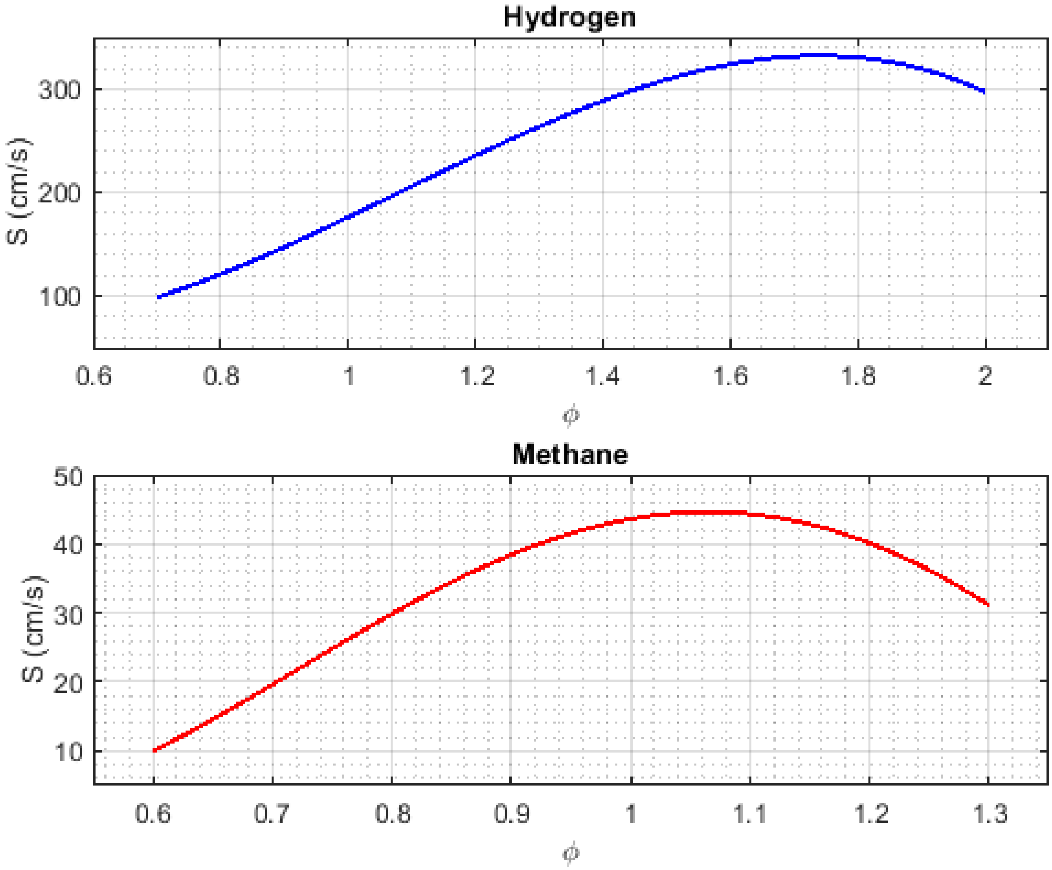

Figure 3.5: Burning velocity fuel-air mixture at T=300 K and p=1 atm

Fig.3.5 shows that the laminar burning velocity is approximately equal to $1 \div 3$ m/s for hydrogen and $0.1 \div 0.5$ for methane mixture. These velocities are much less than the speed of sound values for the same mixtures (Sec.1.2, fig.1.4), so it's clearly evident the subsonic nature of the phenomenon. In particular, the maximum laminar burning velocity does not occur at stoichiometric composition but at fuel-rich mixtures ($\Phi \sim 1.8$ for hydrogen and $\Phi \sim 1.1$ for methane).

Velocity values are also influenced by the adiabatic flame temperature (and so fuels with high heats of combustion tend to propagate a flame faster) and by the diffusive nature of the fuels [35]. Therefore in fuel-oxygen systems the burning velocity is much higher because of the greater heat released during the reaction and the larger reaction rates.

Eq.3.25 is correct only for laminar case in which heat transport happens by molecular conductivity. In turbulent case the thermal conductivity k is higher, so the flame front propagates faster at turbulent speeds S_T which are usually $10 \div 100$ greater than laminar velocity. This occurs because turbulence makes easier the transfer of heat from the ignition source to the sorrounding layer.

3.3.2 Pressure Change

The pressure variation through the flame can be estimated using the continuity mass and momentum equation for the one-dimensional case (eq.3.12-3.13).

Momentum equation permit to evaluate the change in pressure $p_u - p_b$ between downstream and upstream of the wave:

$$p_u - p_b = \rho_b S_b^2 - \rho_u S_u^2 \tag{3.26}$$

in which "u" and "b" stay for "unburned" and "burned" and so S_u represents the burning velocity. For continuity equation $\rho_u S_u = \rho_b S_b$, so:

$$p_u - p_b = \rho_u S_u \cdot (S_b - S_u) \qquad \Rightarrow \qquad p_u - p_b = \rho_u S_u^2 \cdot (\frac{S_b}{S_u} - 1) \tag{3.27}$$

Again, for the mass conservation equation, $\frac{S_b}{S_u} = \frac{\rho_u}{\rho_b}$ therefore the final expression for pressure change is the following:

$$\boxed{p_u - p_b = \rho_u S_u^2 \cdot (\frac{\rho_u}{\rho_b} - 1)} \tag{3.28}$$

Since $\rho_b < \rho_u$ because of temperature increase, even $p_b < p_u$ hence there is a drop in pressure.

Tipically: $\frac{\rho_u}{\rho_b} \sim 6$; ρ_u is equal to $\sim 0.85\, kg/m^3$ for hydrogen mixtures and $\sim 1.15\, kg/m^3$ for methane mixtures; S_u is about 2 m/s and 0.4 m/s for hydrogen and methane respectively (fig.3.5). With these values the pressure variation for hydrogen and methane mixtures is about $\Delta p = 1 \div 20$ Pa which are very small values. For this reason the pressure can be considered almost constant and that's why c_p has been used in the previous discussion.

Chapter 4

Detonation

A detonation represents the sonic or supersonic propagation of a combustion-driven shock wave in an unreacted medium. The shock wave compresses the unburned mixture resulting in an increase of temperature above the auto-ignition temperature. So behind the shock chemical reactions occur and the energy released by them sustains the propagation of the wave. For example, consider an explosive gas mixture and a source of energy is deposited impulsively inside it. The release of energy in a short period of time can generate a shock wave which intensity and velocity decay with distance (*blast wave*). If the wave is strong enough, very high values of temperature and pressure can be reached and chemical reaction can be induced behind the shock. Therefore a detonation wave is essentially a reagent shock wave in which the chemical reaction front and the shock front are coupled. Unlike deflagrations, the ignition of the mixture in detonations is mainly due to adiabatic compression of the gases and the consequent reactions in turn drive the wave sustainig it.

4.1 C-J Detonation

The first theory to study the features of a detonation wave in a gas was developed by Chapman and Jouguet and so it is called Chapman-Jouguet (C-J) theory. This theory allows to calculate the detonation velocity of an explosive mixture; indeed, detonations have a unique and costant propagation velocity.

C-J theory assumes detonation wave as steady, planar and one-dimensional and does not require any information about chemical kinetics. For given initial conditions, two possible solutions exist for a detonation wave: strong and weak detonation (fig.3.3). In the first case, the velocity of the flow downstream the wave is subsonic while in the second is supersonic. The two solutions converge when the detonation velocity is a minimum and no detonation occurs below it [36]. Above this minimum, Chapman and Joguet provided a criterion to pick out the correct velocity among all the possible solutions.

From experimental tests Chapman deduced that the correct velocity was the minimum one ([9]), while according to Jouguet it was the one that gave a minimum entropy across Hugoniot curve ([30]). Both their thesis were right: infact it has been shown later that for a given mixture the correct velocity for a steady-state detonation is the minimum velocity which also corresponds to the minimum entropy, and it is known as Chapman-Jouguet velocity. Moreover, it can be demonstrated that C-J velocity is such that the velocity of the products behind the wave is equal to the sound speed in the products, thus the gases downstream the wave have M=1 [23]. This means that the disturbances, due to the gas expansion behind the wave, can not catch up with the detonation front and so the wave will travel to a constant velocity. This condition and the other physical ones are called C-J conditions. They are depicted on Hugoniot curve (fig.(3.3)) by the C-J point, i.e. the point in which the Hugoniot curve and the Rayleigh line are tangent. From the tangency of the two curves, it is possible to evaluate an analytical expression for the C-J velocity [35]:

$$\boxed{V_{CJ} = \sqrt{2(\gamma^2 - 1) \cdot q}} \tag{4.1}$$

Where γ has been assumed equal ahead and behind the detonation. Hence, knowing the heat release by combustion, eq.4.1 allows to calculate the unique propagation velocity for a steady detonation wave.

For strong detonations, the propagation velocity is higher than C-J velocity, so it might seem that detonation waves don't have a unique velocity. Actually, since in region I of fig.3.3 pressure behind the wave is higher than C-J case, the velocity of the products is lower than speed of sound, which means that the flow is subsonic after the detonation. Then the disturbs can reach the front and the detonation will start to decay. In this case, detonation wave is not steady and it is used to be called as ”Overdriven detonation”; nevertheless its velocity will keep on decaying until it gets stationarity conditions and it will continue propagating like a C-J detonation. Instead, pressure in region II is lower than C-J pressure and the velocity of the downstream products is greater than the speed of sound, therefore the flow is supersonic. In practise this situation is not possible since in a normal shock wave the downstream flow must be subsonic.

It is good to emphasize that C-J theory is not based on strict physical arguments but it just provides a criterion to evaluate the correct detonation velocity for an explosive mixture.

4.2 ZND Models

The simplest 1-D model which takes into account the reaction rate was developed independently by Zeldovich [56], von Neuman [53] and Doring [17] by 1940s.

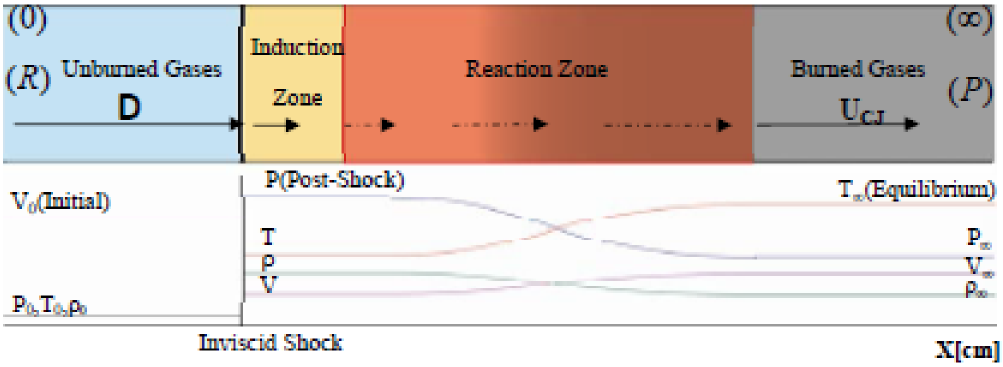

Figure 4.1: ZND structure [42]

Fig.4.1 shows the detonation structure and the qualitative trend of pressure, temperature, density and velocity inside the different regions. Ignition of the reactants is due to the adiabatic compression of the leading shock wave which causes a sharply increase of pressure, temperature and density; instead, the gas velocity passes from supersonic to subsonic values.

After the shock wave, the gas conditions are such that chemical reactions can start, but they need an ”induction time” to occur or equivalently a small distance

Δ_i called induction zone where the different quantities remain almost constant and no reactions occur (Sec.2.3.4).

In the reaction zone, chemical reactions happen and heat is released, so temperature, pressure and density change until they get to C-J equilibrium condition. More in detail, temperature in the reaction zone continues raising because of the heat produced by the exothermic recombination reactions while pressure and density fall until C-J values: in particular, the gas expansion exactly sustains the leading shock propagation. As density decreases, flow velocity must increase for the mass conservation ($\rho u = cost$) and it can be demonstrated that the final equilibrium gas velocity U_{CJ} at the end of the reaction is approximately equal to the speed of sound of the local mixture [23, 36].

4.3 Detonation Front Structure

While ZND theory assumes detonation wave as a one dimensional structure, actually the detonation front is not smooth but it is a three-dimensional frame constitued by multiple shocks. Infact, transvers shocks are present and their interaction with incident shocks wave results in the formation of Mach stem and *triple point*, in which the three kind of shock intersect.

Triple point trajectories cause the detonation propagation to occur through a characteristic structure, known as detonation cell, reported in fig.4.2. Each cell is characterized by its width λ, which is a useful parameter because it is related to the energy required to start reactions and to the reaction zone length. It has been proved that the more reactive are the gases, the smaller is λ, therefore as λ grows even the activation energy required increases [23]. Since λ strongly depends on composition, usually its lower value occurs at stoichiometric composition to which precisely energy needed is less.

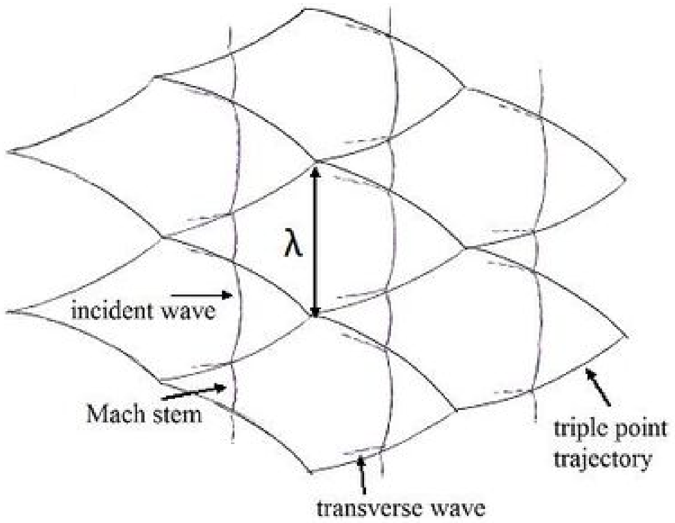

Figure 4.2: Detonation Front Structure [15]

The presence of multiple shock makes the front unstable and very complex. Mach stem shock is usually stronger than incident shock, therefore the induction time behind the incident shock is greater than behind Mach stem. This causes turbolences and the presence of slip lines to separate flow at different conditions.

In addition, the reaction zone changes along the cell: at the beginning it is coupled with the Mach stem originating at the triple point, since they propagate at velocities upper than C-J. Progressing to the cell, the Mach stem weakens and the wave turns into a incident shock (greater induction time) resulting in a progressive distancing of the reaction front from the shock [47].

4.4 Detonation Initiation

A detonation wave can be initiated essentially in two ways. The first one is faster and it is possible if a big quantity of energy is provided to an explosive mixture. This energy source can be an electric spark, an explosive or an external strong shock wave; for example, such a wave might be generated by explosive charges: it has been tested that 10g of C-4 explosive can initiate a detonation in an hydrogen and air mixture (with 30% hydrogen)[26].

The second mode is slower than the previous one and it is a tranisition from a deflagration wave. Turbolence and interactions between pressure waves and flame are the key-factors in flame acceleration and detonation beginning. These two situations are respectively known as "*direct initiation*" and self-ignition or *"Deflgration-to-Detonation transition"* (DDT).

4.4.1 Direct Initiation

Direct initiation consists in the achievement of the critical conditions for detonation onset "instantaneously", i.e. without the flame acceleration step. Direct initiation can be obtained through different means: strong shock wave, turbulent jet of hot products (for example in cavitation, see later), jet of reactive species etc. Among all the different mechanisms, the simplest one to study is maybe the "blast initiation".

This process was initially studied in the context of sperichal detonation formation in unconfined space, in which a DDT mechanism is quite improbable. To have a detonation, the igniter must be capable to form a strong shock wave which has to keep a minimum strength for some necessary time. At the beginning the energy source generates a blast wave which is much stronger than C-J detonation for that particular mixture; then the blast wave expansion causes it to decay, the chemichal energy released influences its propagation and the initial blast wave forms an overdriven detonation; far from the igniter, if the initial source is strong enough, it asimptotically tend to a C-J detonation [36].

Depending on the igniter energy, three regimes can be obtained: subcritical, critical and supercritical. In subcritical regime the initial energy is below a certain threshold, so it cannot produce a durable detonation; reaction front and blast wave progressively separate and after the decoupling the first one carries on as a flame and the second as a sound wave. For energies above the threshold, i.e. in the supercritical regime, blast wave forms initially an overdriven detonation and later it decays to a C-J detonation. In this case, reaction front and blast wave are coupled for all the propagation. Critical regime, instead, is more complex and a quasi-steady period is observed. This period corresponds to an initial decay of the blast wave and its decoupling from the reaction front as well as in the subcrtical regime, since in the first moments blast energy completely regulates the blast motion.

At the end of the quasi-steady period, local explosions occur in the reaction front; they initially give rise to detonation ”bubbles” which grow up and form an asymmetrical detonation [36, 38].

Many studies have been conducted to evaluate the critical initiation energy. In general all the detonable mixtures show a similar dependance of the critical energy on equivalence ratio (composition) which can be represented as a U-shape curve. The minimum of the curve, which corresponds to the minimum critical energy, is at stoiciometric ($\Phi = 1$) while it tends to infinite values near particular fuel-concentrations called *detonability limits*.

Zel’dovich [54] was the first to postulate a criterion for connecting critical energy to the chemical properties of a mixture. Chemical reactions need an induction time in order to release energy for shock wave support. Since blast wave progressively decays and the time for the blast wave to decay depends on the initial energy, Zel’dovich criterion hypothesizes that the energy to direct initiation must be such that induction time and decay time are at least equal. Applying this criterion he demonstrated that the critical Energy E_0 is proportional to the cube of the induction time for spherical detonation (eq.4.2):

$$\boxed{E_0 = 125\pi\rho_0 I a_0^5 M_{CJ}^5 \tau_{ind}^3/2} \tag{4.2}$$

in which I is a constant depending on heat capacity ratio γ, a_0 and M_{CJ} are respectively the speed of sound in the unburned mixture and the Mach number of the C-J detonation.

Other general theories have been proposed for the critical energy evaluation like the ”detonation kernel” theory by Lee [38]. Because of the induction time, chemical reactions to take place need a minimum distance R_s^*, called detonation kernel, at which the decaying blast wave reachs a critical Mach number M_s^* corresponding to a rapid autoignition of the gases behind the shock. If R_s^* is too small, the chemical energy released is neglectable compared to the igniter energy which dominated the phenomenon, resulting in a progressive blast decay.

Developing the theory, from knowledge of the autoignition condition (M_s^* and $\tau_{ind}(M_s^*)$), the detonation kernel R_s^* can be obtained, and consequently the critical energy for spherical detonation can be calculated (eq.4.3 is taken from "*Initiation of Gaseous Detonation*" by Lee [38]) :

$$E_0 = \frac{4\pi\rho_0 a_0 {R_s^*}^3}{2} \cdot \left[{M_s^*}^2 I - \frac{1}{3\gamma(\gamma-1)} \right] \tag{4.3}$$

As expected, eq.4.3 shows that initiation energy is proportional to the the cube of R_s^* which is directly related to the induction time. Using the equation, it is possible to get an idea on the critical energy required to direct detonation for hydrogen and methane mixtures. Anyway data taken from Caltech Database points out that very high energies are required to initiate a detonation directly (tab.4.1):

Table 4.1: Critical energy required for direct detonation [31]

STOICHIOMETRIC MIXTURE	CRITICAL ENERGY (J)
$H_2 - O_2$	2
$CH_4 - O_2$	~ 60
H_2-Air	~ 4000
CH_4-Air	$\sim 1 \cdot 10^8$

Clearly the critical energy for fuel-air mixtures are $3 \div 6$ orders of magnitude greater since $E_0 \sim \tau_{ind}$ and, infact, induction time is much higher in fuel-air detonations.

Obviously the previous theories don't consider the three-dimensional structure of a detonation wave. Introducing the cell width λ, some equation to relate the critical energy to λ can be derived [37]:

$$E_0 = 500\pi\rho_0 I V_{CJ}^2 \lambda^3 \tag{4.4}$$

$$E_0 = (2197/16)\pi\rho_0 I V_{CJ}^2 \lambda^3 \tag{4.5}$$

As discussed in Sec.4.3 the initiation energy strongly depends on λ: the greater is the cell size the greater is the energy required to a start detonation.

4.4.2 Deflagration-to-Detonation Transition

An explosive mixtures can support both deflagrations and detonations. Unlike deflagrations, detonations propagate at a specific and costant velocity (Sec.4.1). Under certain conditions, since the deflagration state is not well defined and intrinsically unstable, it is possibile for the flame to accelerate up to the higher detonation velocity. This mechanism of detonation initiation based on flame acceleration is called Deflagration-to-Detonation Transition (DDT).

DDT process can be divided in two phases: flame acceleration and onset of detonation. In Sec.3.3.1 the burning velocity for a 1-D planar flame has been defined as the flame front velocity along the propagation direction. Actually, consider for example a mixture inside a tube, the flame is a 3-D structure, and its three dimensionality has to be taken into account. Flame acceleration is thus referred to the volumetric burning velocity which is obtained multiplying the burning velocity with the cross-section area of the tube. Any mechanism, such as instabilities, turbulences or fluctuations, causing a transition from a laminar to a ”turbulent” structure, induces an increase in the surface area. This consequently produces an increase in the volumetric burning velocity [36].

The geometry also play an important role in this acceleration step because the confinement of the gas in a closed space such as tubes, pipes, vessel etc., generates turbolences. For this reason it is more difficult to have a DDT in a completely unconfined environment, since there would not be any obstacles with which the flame can interact.

An other key-factor is the formation of pressure waves. When flame starts accelerating, the precence of walls and obstacles results in the genesis of pressure waves whose interaction with the wall and the flame front is one of the main causes of turbolences [49]. Furthermore the passage of a pressure wave causes an increase in temperature of the mixture, therefore the successive waves propagate faster (the mixture is warmer so the speed of sound is higher) and they can catch and pack giving origin to a shock wave.

Due to the variety of mechanisms and parameters that have to be considered in flame acceleration, DDT can occur in different ways and a specific theory is impossible to develop. Anyway, in the last phases of flame acceleration, the flame front appears totally distorced, forming a ”brush” flame. This pre-detonation regime ends when ”critical condition” to detonation onset are reached. Detonation onset in not a countinous process and it usually happens when flame velocity is equal to the C-J deflagration velocity (i.e. the maximum possible velocity for a deflagration) that is of the order of the half C-J detonation speed. In this condition the flame becomes more and more corrugated until it is able to engulf the unburned gas giving origin to localized ”explosion in the explosion” (defined in this way by Oppenheim) which lead to the formation of ”hot spots”. These hot spots or explosion centers produce a blast wave which evolve in a detonation bubble and after in a overdriven detonation [36, 38]. The distance from the initial flame to the detonation onset is called *run-up distance*.

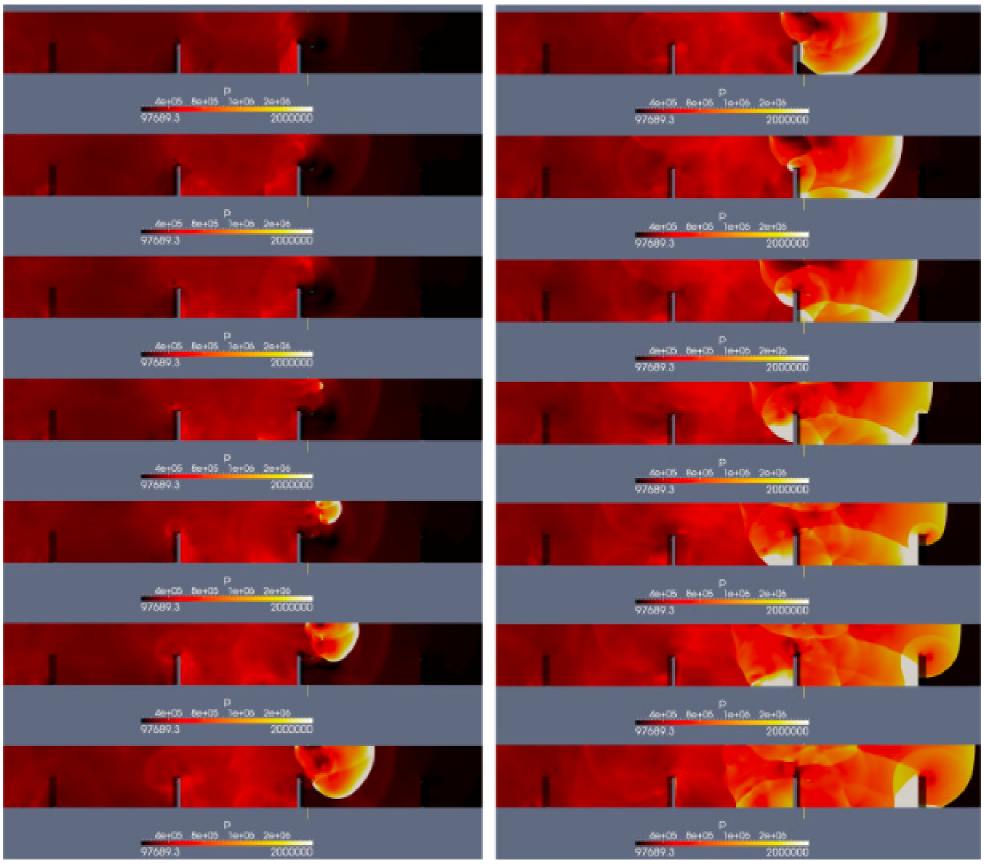

Figure 4.3: Onset of detonation [27]

That described is the most common mechanism in detonation waves formation and it can be observed in fig.4.3 that is the outcome of an experiment carried out with an hidrogen/air mixtures ignited in a 80 mm × 2000 mm shock tube.

Fig.4.3 illustrates the pressure field: at the beginning the pressure waves are weak even if they collide continously. In the 4th left picture the first hot spot appears and subsequently it expands until a detonation wave is formed [27].

Other experimental tests about hydrogen [18, 40] and methane [33] mixtures are available in literature. In general it is easier to have self-ignition (DDT) in fuel-oxygen mixtures rather than fuel-air because of the higher laminar flame speed. In the fuel-air mixtures the flame speed is in the order of 0.5 m/s and so it is required a greater amplification to reach the conditions for the detonation onset.

As seen in Ch.2, the energy required to ignite a methane or an hydrogen mixture is a fraction of some milli Joule, whereas in Sec.4.4.1 it has been said that the direct initiation of a detonation needs a huge amount of energy. It is then clear that having a deflagration is much easier than a detonation. For this reason in the most of the accidental explosion DDT appears the most probable cause of detonation initiation.

4.5 Two-phase detonation

In most of aerospace applications, propellants are used in the liquid state, therefore the understanding of liquid detonation is important as well as gaseous detonation. Flammable liquid spilling can be as dangerous as gas leak, because liquid propellants can produce vapour or two phase mixtures, which may explode if dispersed in an oxidant. Since detonation in single-phase and two-phase mixtures is quite different, a brief overview is presented. In general liquid fuel detonation is much more complicated than gaseous one because a lot of factors have to be taken into account. About that, many studies about aerosol or spray mixtures have been conducted. An aerosol (spray) is a two-phase mixture in which liquid droplets are dispersed in a gas. Droplets can be formed by liquid atomization due to a nozzle or a injector, or by splashing on a surface.

Experimental tests have shown that in two-phase mixtures, constitued by gaseous oxygen and fuel liquid droplets, propagation velocity is lower than theoretical C-J velocity and the greater is the droplet size the greater is the difference. Moreover the interaction between the shock wave and the droplet causes its breakup. Therefore the time required to break the droplet results in a greater reaction zone [14].

Droplet size play an important role even in the propagation mechanism: for droplets below $10 \mu m$ aerosol detonation is similar to that of gaseous mixtures, as droplets completely evaporate and form a vapour mixture. Droplet evaporation is an important factor too, because it results in an increase of combustible gas density and consequently in an increment of combustion products pressure. Larger droplets, instead, don't have enough time to completely vaporize; therefore each droplet burns alone and droplet breakup is necessary to sustain detonation. In this case a sensitive difference in propagation velocity compared to C-J velocity is present.

Other researchs have shown that a minimum precence of vapour is necessary for detonating liquid fuels, and in high-volatility fuels is much simpler to initiate a detonation [7].

In conclusion, it can be affirmed that liquid fuel detonation depends on many parameters such as droplet atomization, droplet size and density, propellants volatility etc. and, in addition, experimental tests have shown that aerosol mixtures can sustains very strong detonation because of the propellant concentrations. Moreover the presence of liquid droplets, which are already more unstable than gaseous particles, increases turbolence and instabilities helping in deflagration to detonation transition. So even a small heat source can ignite the mixture and then give origin to fast deflagrations and detonations [46].

4.6 Summary

Deflagrations and detonations can be differentiated in many ways. Deflagration is an expansion wave that propagates at subsonic velocity. It is controlled by heat and mass diffusion from the reaction zone to the unburned mixture. On the other hand, detonation is essentially a regent shock wave that ignites a mixture by adiabatic compression. It moves through a mixture at a unique velocity unlike deflagration. Because of its lower initial energy for starting reactions, it is simpler to have a deflagration rather than a detonation, but, being particularly unstable, it can easily accelerate and transform into a detonation.

In the next table the most important explosive characteristics discussed in the previous chapters of hydrogen and methane are reported.

Table 4.2: Hydrogen and methane Combustion properties [16]

Property	*Hydrogen*	*Methane*
Heat of combustion (kJ/mol)	-286	-889
Flammability Limits (% in oxygen)	$5 \div 95$	$5 \div 61$
Flammability Limits (% in air)	$5 \div 75$	$5 \div 15$
Minimum Ignition Energy (MIE) (mJ)	0.02	0.29
Autoignition Temperature (AIT) in oxygen (C)	560	556
Autoignition Temperature (AIT) in air (C)	572	630
Adiabatic Flame Temperature in oxygen at stoich. (K)	3070	3040
Adiabatic Flame Temperature in air at stoich. (K)	2300	2100
Burning Velocity (m/s)	$2.7 \div 3.4$	$0.036 \div 0.48$
Critical Energy for direct det. at stoich. in oxyg. (J)	2	60
Critical Energy for direct det. at stoich. in air. (J)	4000	$1 \cdot 10^8$
Detonation Velocity (m/s)	$1500 \div 2200$	$1400 \div 1800$
Energy of explosion (kg TNT 10^{-6} Btu)*	170	220

*The energy of explosion is often quantified by comparing it with a reference quantity. Usually it is TNT because of the huge number of experimental tests conducted on this explosive. Therefore the energy of explosion in the last line of tab.4.2 has been evaluated with the *TNT equivalency method.* It represents the mass of TNT which could produce the same explosion energy of the considered mixture. To do this, first of all it is necessary to convert the mass of the mixture in an equivalent mass of TNT:

$$m_{TNT} = \frac{\eta m \Delta H_c}{E_{TNT}}$$

where η is the empirical explosion efficiency [13] and E_{TNT} is the TNT explosion which is universally recognized to be equal to 1120 cal/g.

Chapter 5

Analysis

In this chapter some examples about hydrogen and methane ZND detonations are presented. The following simulations implement the theory and the equations discussed in Sec.3.1.1. They have been carried out with the numerical routines of the "Shock & Detonation Toolbox" implemented in Matlab [6, 4]. The SD Toolbox uses the Cantera open-source software, created at Caltech by D. Goodwin, which provides suitable tools to simulate and solve problems involving chemical kinetics, thermodynamics and transport process [25]. To simulate the behaviour of a gas mixture crossing a detonation wave, an appropriate reaction mechanism is necessary. Here the GRI 3.0 mechanism by Gas Research Institute has been adopted. GRI 3.0 is a tested mechanism which contains 325 reactions and 53 species [51], including hydrogen and methane combustion/detonation chemical reactions discussed in Ch.2.

For a given mixture at known conditions (temperature, pressure, composition etc.), the program first evaluates the post-shock state, as discussed in *"Numerical Solution Methods for Shock and detonation Jump Conditions"* [5] which is then used as initial condition to solve iteratively the ZND governing equations [4], evaluating in this way the behaviour of the different mixture properties through the wave. It has been chosen to use the C-J velocity as detonation propagation speed in all simulations. ZND is a 1-D steady model, so the analysis show the evolution of the planar detonation wave in function of the spatial coordinate along which propagation takes place. They can be representative of detonations in unconfined spaces.

5.1 Hydrogen detonation analysis

The main differences about hydrogen-oxygen and hydrogen-air system detonations are pointed out in the next parts.

5.1.1 Hydrogen-Oxygen

In fig.5.1 the ZND structure of Hydrogen-Oxygen detonation is illustrated. The components of the mixture are in stoichiometric ratio at initial standard condition (p=1 atm, T=300 K).

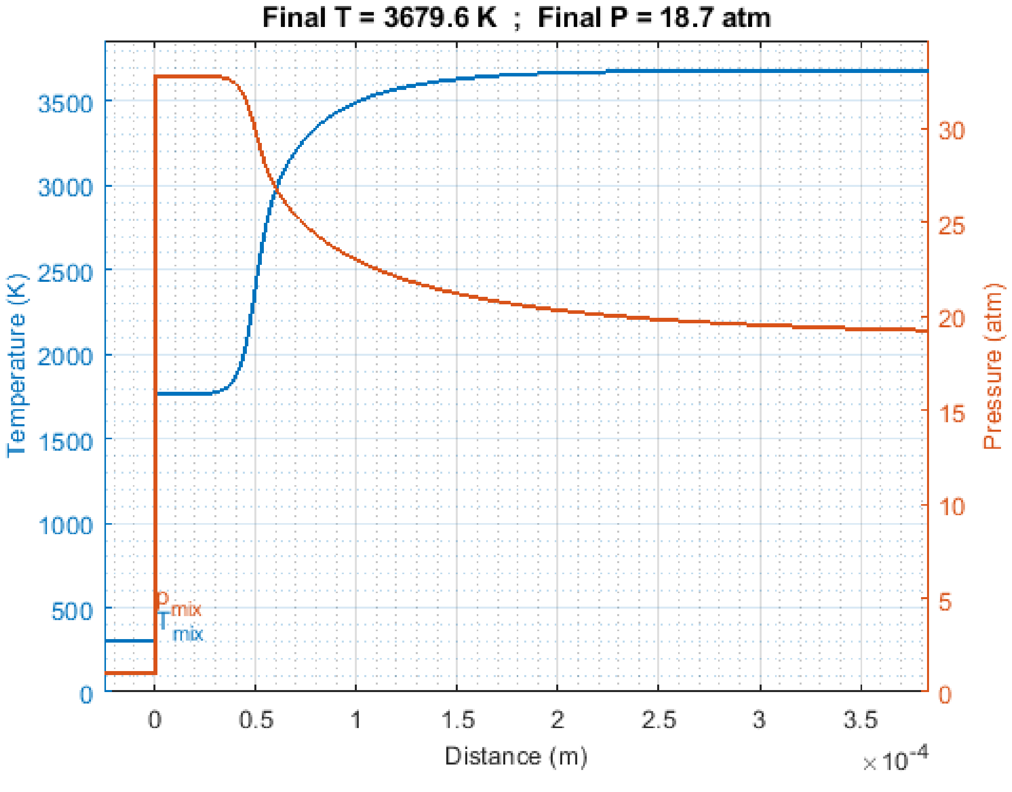

Figure 5.1: ZND structure for $H_2 - O_2$ stoichiometric C-J detonation at p=1 atm and T=300 K. C-J velocity = 2836.4 m/s

The different properties reach their maximum values at the Von Neuman state, i.e. the post-shock state for the C-J case. Immediately behind the leading shock wave an induction zone is present. Here the reaction rates are still low, so the temperature increases slowly. Then, when a large amount of radicals has been produced in the reaction zone, reactions became very fast and the mixture explosive.

This situation can be observed in fig.5.2 in which the production/destruction of the different chemical species in the recation zone is illustrated. At the end of the induction zone, free radicals OH are in higher concentration, therefore temperature rises until it gets to the C-J equilibrium condition where H_2O is obtained as product. Regarding the pressure, after the shock the flow expands, so the pressure decreases and, at the end of the reaction zone, it is equal to the C-J pressure. The time-scale of this phenomenon is extra small as well as the space-scale: infact the induction zone is only $\Delta_i = 5 \cdot 10^{-5}$ m.

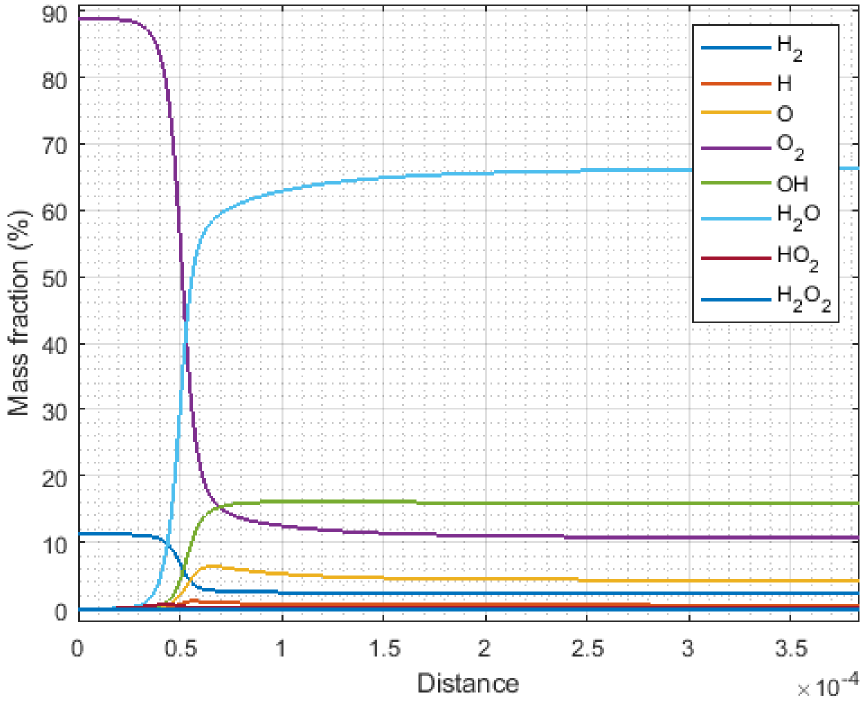

Figure 5.2: $H_2 - O_2$ composition change in the reaction zone

As one expected, mixture velocity and pressure have an opposite behaviour: as the pressure decreases, the flow accelerates up to sonic conditions at the exit (in fig.5.3 the final Mach number of the products is ~ 1).

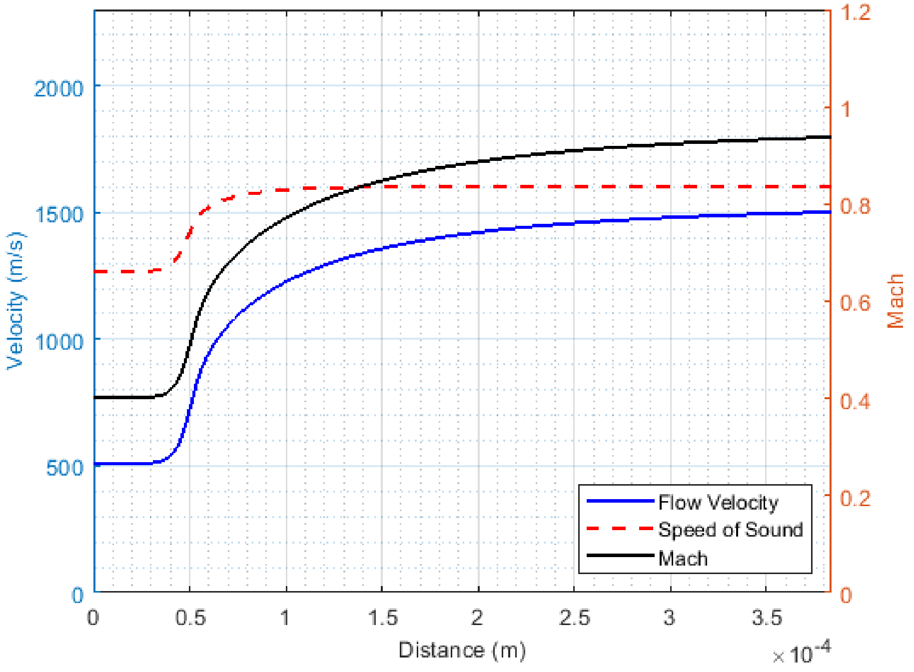

Figure 5.3: $H_2 - O_2$ flow velocity, sound of speed, Mach number of the products in the reaction zone

5.1.2 Hydrogen-Air

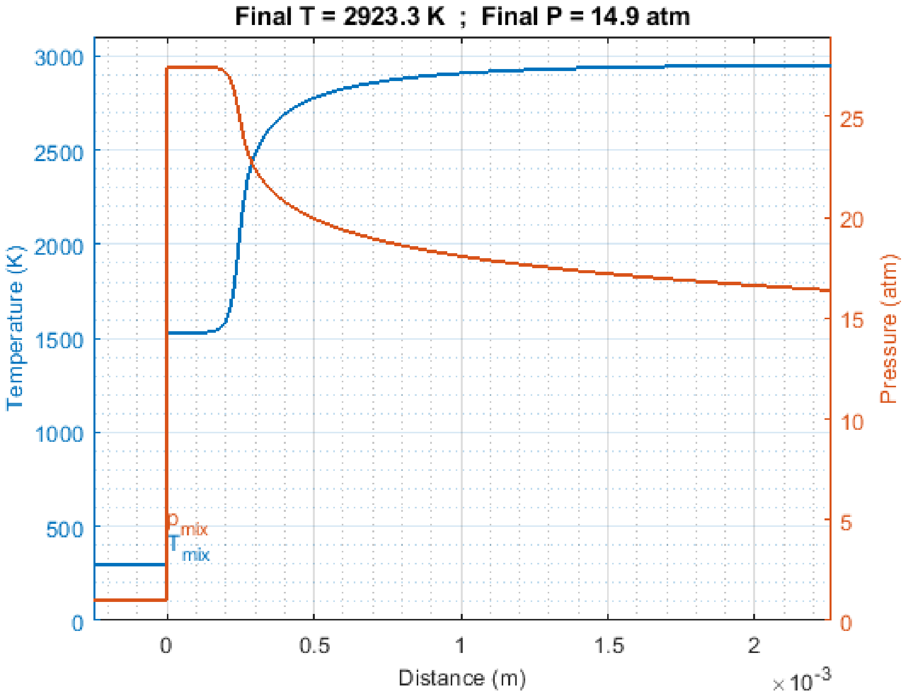

Figure 5.4: ZND structure for $H_2 - O_2$ stoichiometric C-J detonation at p=1 atm and T=300 K. C-J velocity = 1969 m/s

Hydrogen-Air detonation is similar to Hydrogen-Oxygen in physical structure, but in this case the space-scale is much higher ($\Delta_i = 2.45 \cdot 10^{-4}$ m) and all the fluid properties present lower values both after the shock and at the equilibrium (fig.5.4). The lower values are due to the huge amount of N_2 in the air (air is formed of about 79% of N_2).

As fig.5.5 shows, nitrogen does not partecipate to hydrogen oxidation, infact, its variations across the wave are negligible.

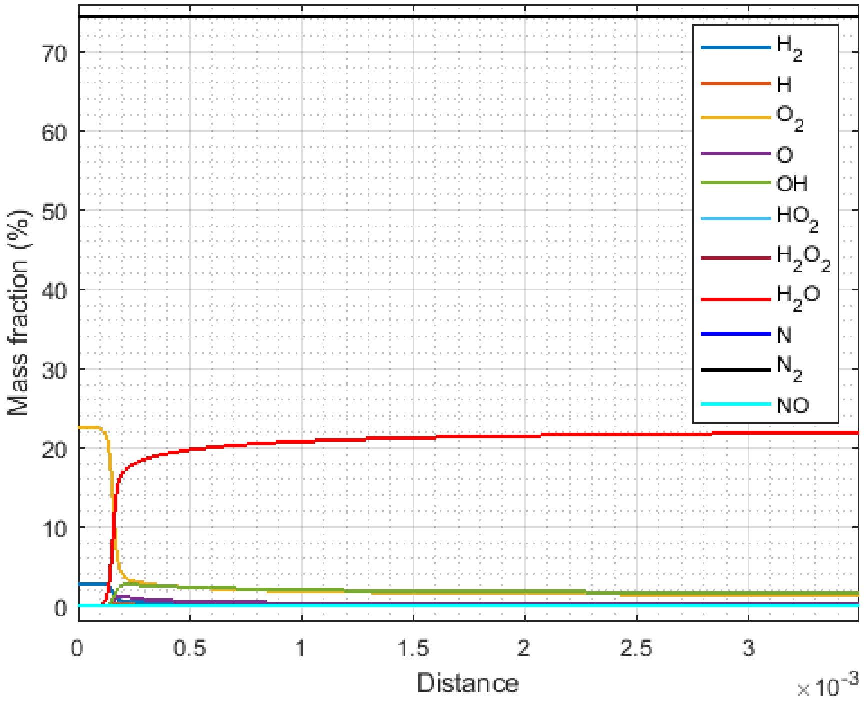

Figure 5.5: H_2-Air composition change in the reaction zone

Finally, it's possible to represent the Rayleigh line and the Hugoniot curves of reactants and products for hydrogen-oxygen and hydrogen-air mixtures (fig.5.6). In particular, the intersection between Rayleigh line and reactant Hugoniot curve provides the VN state while product Hugoniot curve and Rayleigh line are tangent because this is a C-J case.

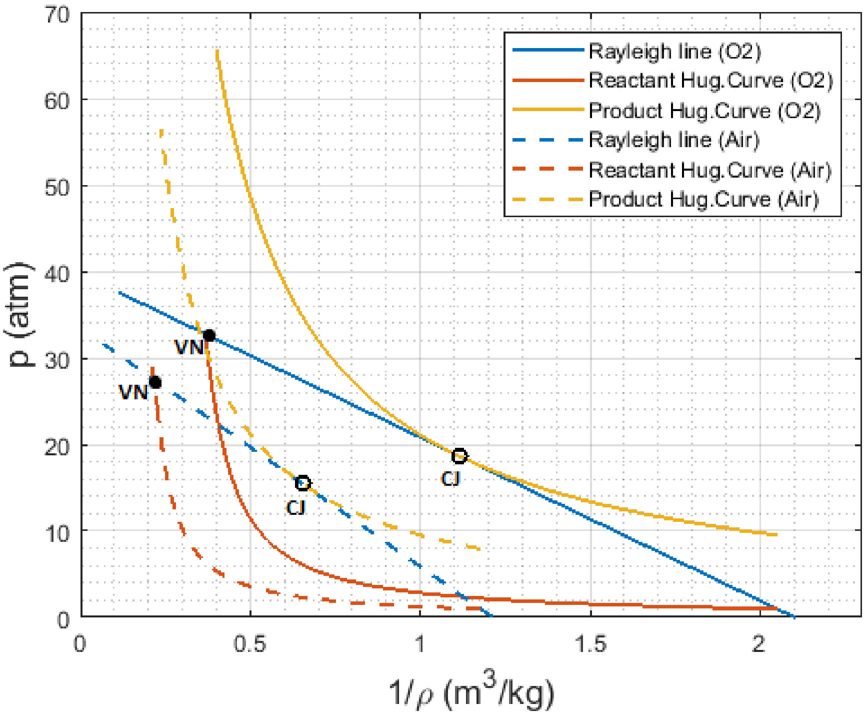

Figure 5.6: Rayleigh line and Hugoniot Curves

5.2 Methane detonation analysis

Reactions involved in methane-oxygen combustion are reported in Ch.2. Using them a similar analysis to that of the previous section is conducted in order to point out methane-oxygen and methane-air mixture detonation differences.

5.2.1 Methane-Oxygen

Temperature and pressure through induction and reaction zone show the same well-understood trend (fig.5.7) similar to hydrogen case. From the analysis, the equilibrium temperature of the products reults to be very close to the corresponding of hydrogen-oxygen system, while the final pressure is quite higher.

In fig.5.8 composition changes inside the reaction zone is illustrated. Unlike hydrogen, methane forms much more species during its dissociation, even if just few of them are reported.

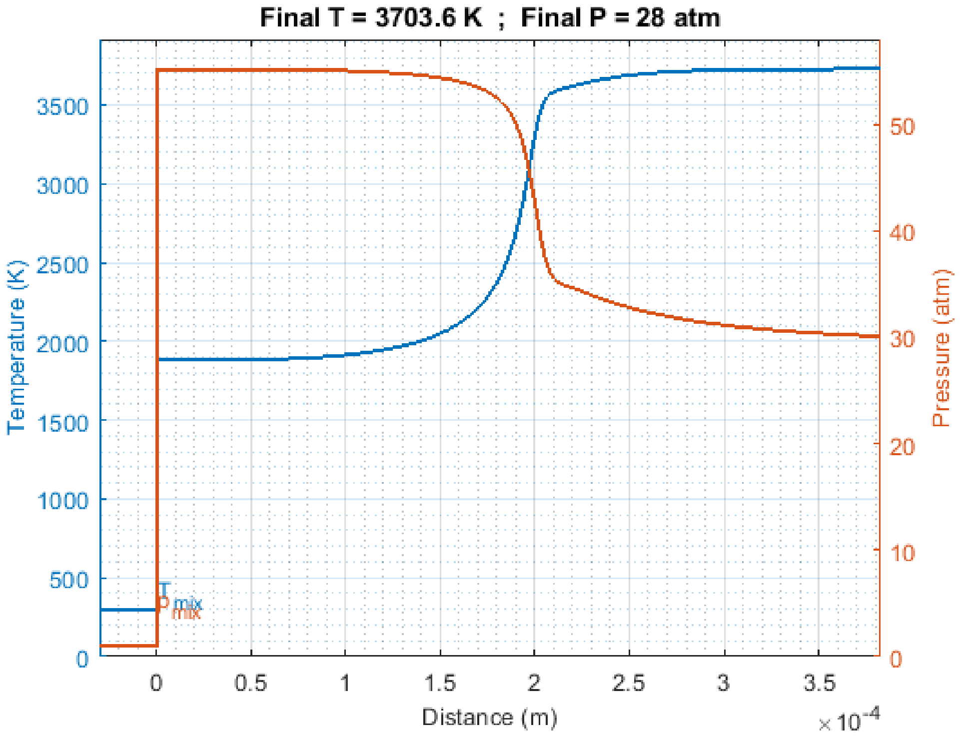

Figure 5.7: ZND structure for $CH_4 - O_2$ stoichiometric C-J detonation at p=1 atm and T=300 K. C-J velocity = 2390.4 m/s

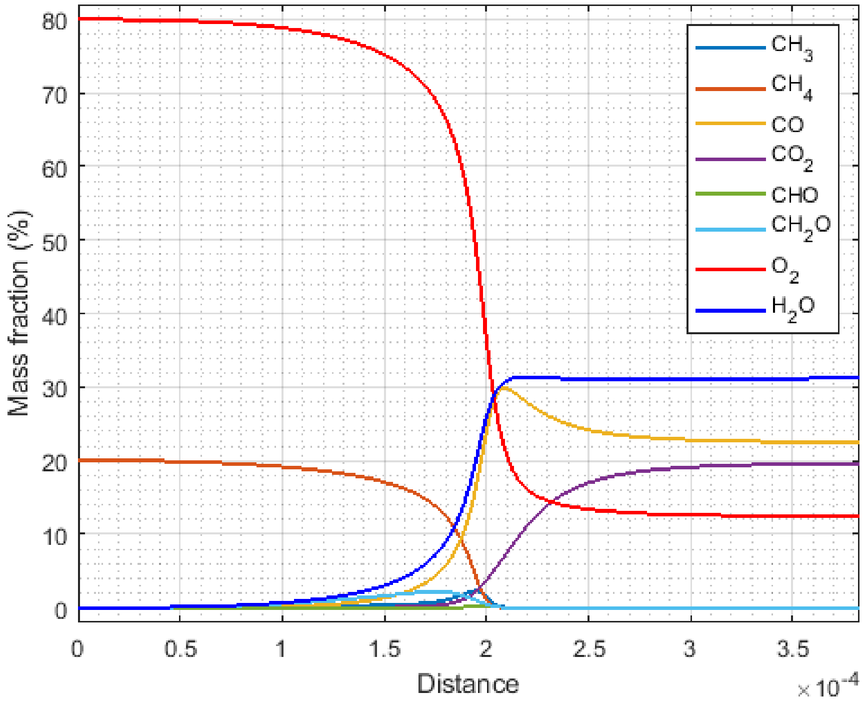

Figure 5.8: $CH_4 - O_2$ composition change in the reaction zone

From fig.5.7 and 5.8, it is possible to observe that temperature starts increasing when CHO radicals are formed (reactions 2.34-2.36). Then temperature exponentially grows up because of the exothermic termination reactions (2.37-2.41) which lead to high carbon-monoxide and carbon-dioxide concentration at the end of the combustion.
Again, as pressure and density decrease in the reaction zone, the velocity of the gas mixture increases as well as the speed of sound (fig.5.9), being this latter proportional to the temperature. As expected the products ate the end of the reaction zone reach sonic condition.

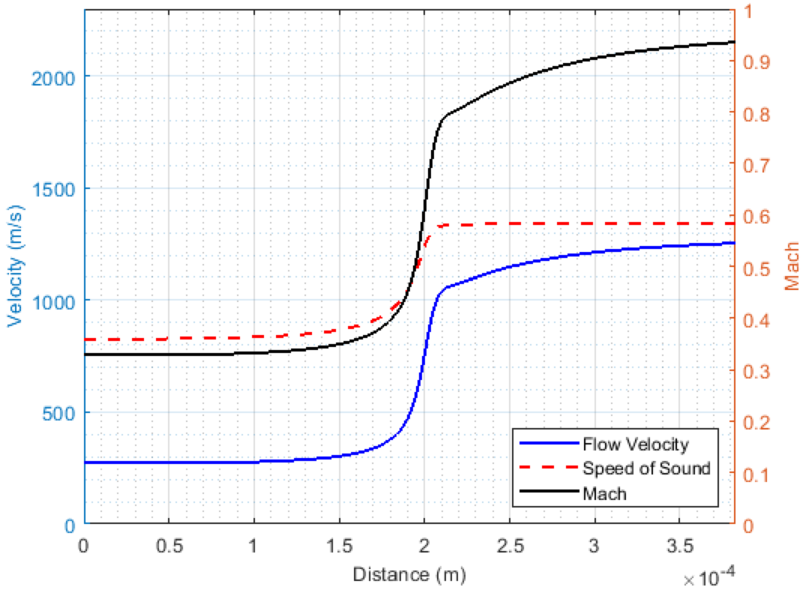

Figure 5.9: $CH_4 - O_2$ flow velocity, sound of speed, Mach number in the reaction zone

5.2.2 Methane-Air

Like hydrogen, also methane-air system has lower values of temperature, pressure, velocity etc. than methane-oxygen mixtures as shown in fig.5.10. Presence of nitrogen results in lower post-shock temperature (almost 500 K compared to methane-oxygen), which causes lower reaction rates and a larger induction zone length ($\sim$ 0.017 m). Once again, only a small quantity of N_2 reacts to form NO_x radicals which subtract heat from the system and this causes a minor equlibrium temperature and less heat released.

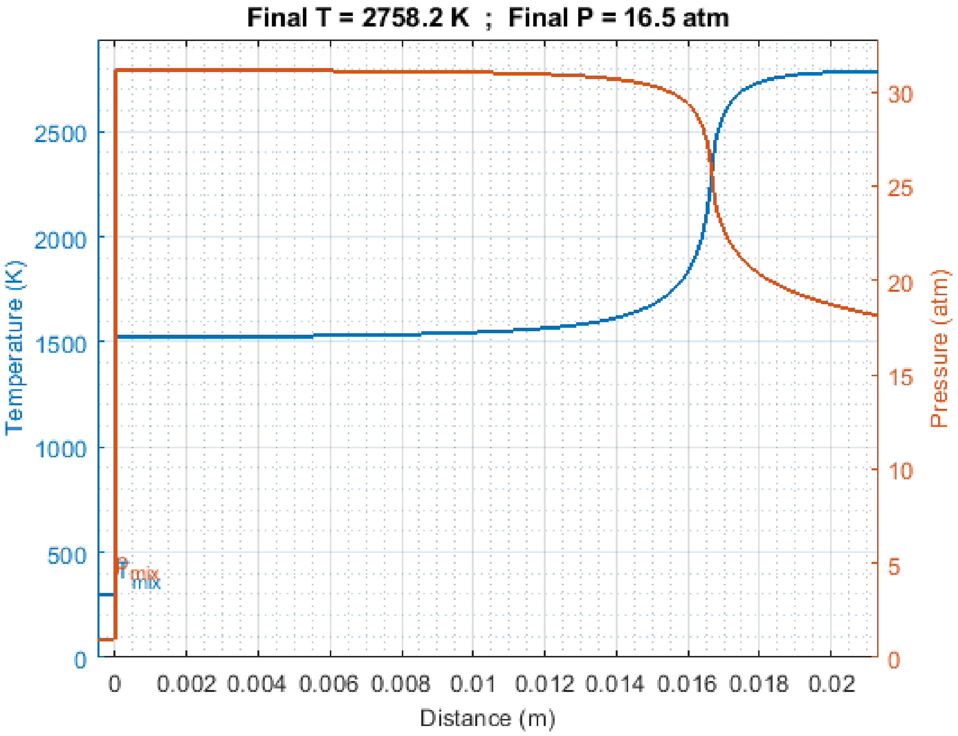

Figure 5.10: ZND structure for CH_4-Air stoichiometric C-J detonation at p=1 atm and T=300 K. C-J velocity = 2390.4 m/s

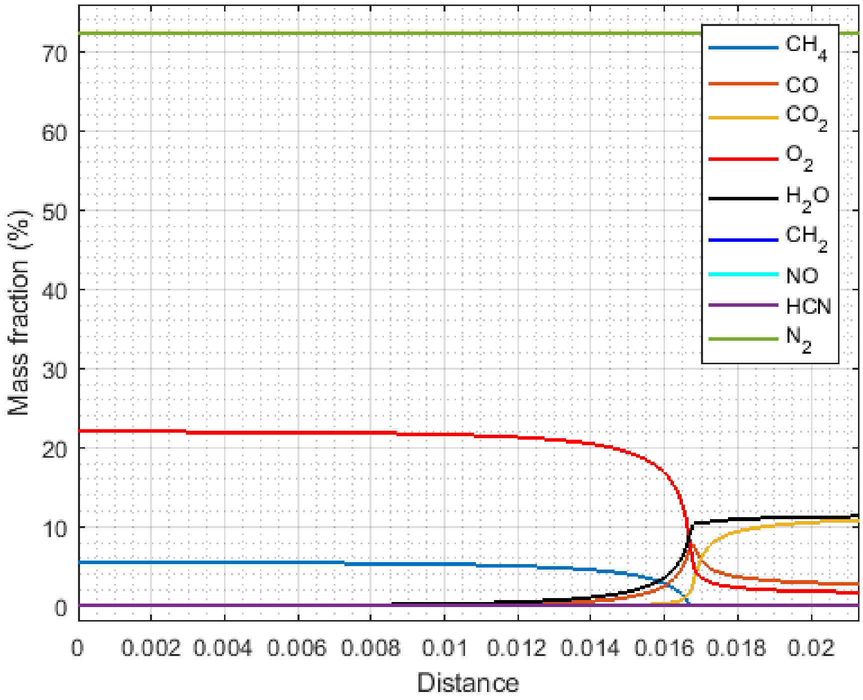

Figure 5.11: CH_4-Air composition change in the reaction zone

5.3 Results and Comments

Tab. 5.1 summarizes the main results from the previous analysis.

Table 5.1: Hydrogen and Methane system's main results

PROPERTY	MIXTURE			
	$H_2 - O_2$	H_2-Air	$CH_4 - O_2$	CH_4-Air
T_{VN}(K)	~ 1800	~ 1500	~ 1900	~ 1500
p_{VN} (atm)	32.8	27.5	~ 60	32.78
T_{CJ} (K)	~ 3680	2923	3703	~ 2760
p_{CJ} (atm)	18.7	14.9	28.0	16.5
Δ_i (m)	$5 \cdot 10^{-5}$	$2.45 \cdot 10^{-4}$	$2 \cdot 10{-}4$	$1.67 \cdot 10^{-2}$
V_{CJ} (m/s)	2836	1969	2390	1803
M_{CJ}	5.2	4.8	6.7	5.1

VN stands for Von-Neuman, i.e. the post-shock state, while CJ for the Chapman-Jouguet equilibrium condition.

Results from tab.5.1 show that detonation waves propagate faster in hydrogen mixtures because of the greater speed of sound, but they have a larger disparity in C-J velocity than methane systems passing from oxygen to air. This is due to the low molecular weight of hydrogen compared to methane and so nitrogen molecules lead to more important changes in density composition of hydrogen systems.

Knowing the speed of sound in the unburned mixture it's possible to evaluate the Mach number of the initial shock wave as $M_{CJ} = \frac{V_{CJ}}{a_0}$. The values obtained clearly point out that in order to have a detonation the leading shock wave must be really strong. Indeed, Mach number varies from a value of 5 to almost 7. Furthermore initial shock wave is stronger in methane mixtures as they require more energy to initiate a detonation.

Detonation waves have different intensities in hydrogen and methane oxygen mixtures, infact temperature and pressure present more marked differences, whereas they are very similar in hydrogen and methane air mixtures. Nevertheless, both in air and oxygen, methane mixtures take more time to reach explosive conditions, indeed the detonation structure has got a larger induction zone than hydrogen. The larger induction zone (and so the greater induction time) is linked to the wide number of intermediate species forming during methane combustion such as CH, CHO, CH_3, CHO, CH_2O etc. and for this reason temperature rises slower. However, all property values are lower for fuel-air mixtures compared to the corresponding in fuel-oxygen systems. Like said before, this is due to nitrogen which does not partecipate to the oxidation mechanism.

Unlike deflagrations, in which pressure drop across the wave is negligible, detonations show pressure increases of about 15-30 times greater than the initial atmospheric value. This is the reason why detonation are much more dangerous and destructive compared to deflagrations.

Presence of nitrogen reduces the energy produced over the entire reaction mainly for two reasons: considering the same volume, the more are the molecules of N_2, the less are those of fuel so the energy density which is released is quite lower; furthermore, a part of the generated heat is absorbed by nitrogen molecules and some NO_x oxidation mechanism occurs. Infact small percentage of $N2$ reacts to form NO_x (NO and NO_2). In particular, during combustion NO_x formation mechanism consists in many elementary reactions depending mainly on temperature and stoichiometric ratio. In hydrogen-air system NO_x is formed exclusively by Zeldovich's thermal mechanism ($T > 1800$ K) [23] and the biggest contribution has nitric oxide (NO). First, the reactive radicals O combine with N_2 (5.1); then the N atoms react through fast reactions with O_2 and OH radicals (5.2-5.3).

$$N_2 + O \Leftrightarrow NO + N \tag{5.1}$$

$$O_2 + N \Leftrightarrow NO + O \tag{5.2}$$

$$OH + N \Leftrightarrow NO + H \tag{5.3}$$

Reactions (5.1)-(5.2) need high energies to be activated, so they subtract heat form hydrogen oxidation process.

Even the propagation velocity is lower (1969 m/s against $\sim$ 2840 m/s), because for eq.4.1 C-J velocity is proportional to the total heat released that is less for hydrogen-air system.

At the same way, NO_x formation during methane combustion results in a less equilibrium temperature and heat released. Unlike hydrogen-air, in methane-air combustion the main NO_x formation mechanism is Prompt mechanism [23]. In this case NO is produced via C species, indeed, during combustion, there are a lot of hydrocarnbon radical that can react with N_2 (5.4-5.6).

$$CH_2 + N_2 \Leftrightarrow HCN + NH \tag{5.4}$$

$$CH + N_2 \Leftrightarrow HCN + N \tag{5.5}$$

$$C + N_2 \Leftrightarrow CN + N \tag{5.6}$$

As a result, HCN, N, CN are easily oxided to NO radicals:

$$HCN + O \Leftrightarrow NCO + H \tag{5.7}$$

$$NCO + H \Leftrightarrow NH + CO \tag{5.8}$$

$$NH + H \Leftrightarrow N + H2 \tag{5.9}$$

$$N + OH \Leftrightarrow NO + H \tag{5.10}$$

Eq. 5.4-5.10 represents the typical prompt mechanism.

It's good to emphasize that all this NO_x reactions play no fundamental role in detonation mechanism. They have been reported to explain the presence of N_2 radicals in fig.5.8 and 5.11, and the lower values in fuel-air systems.

5.4 Effect of composition and initial temperature

5.4.1 Detonation Limits

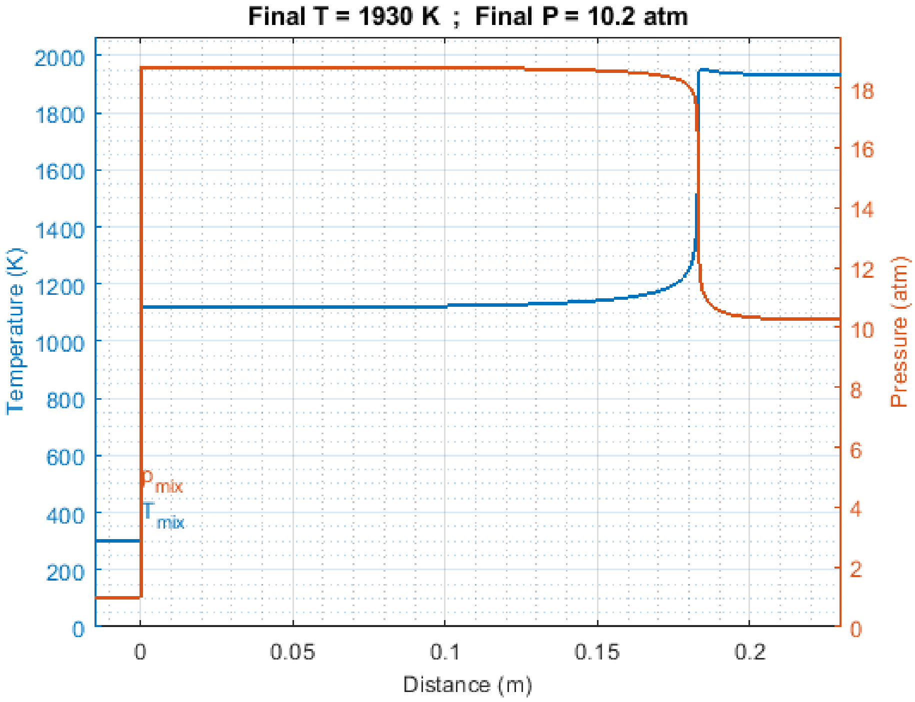

(a) *Lower limit*(15% of Hydrogen)

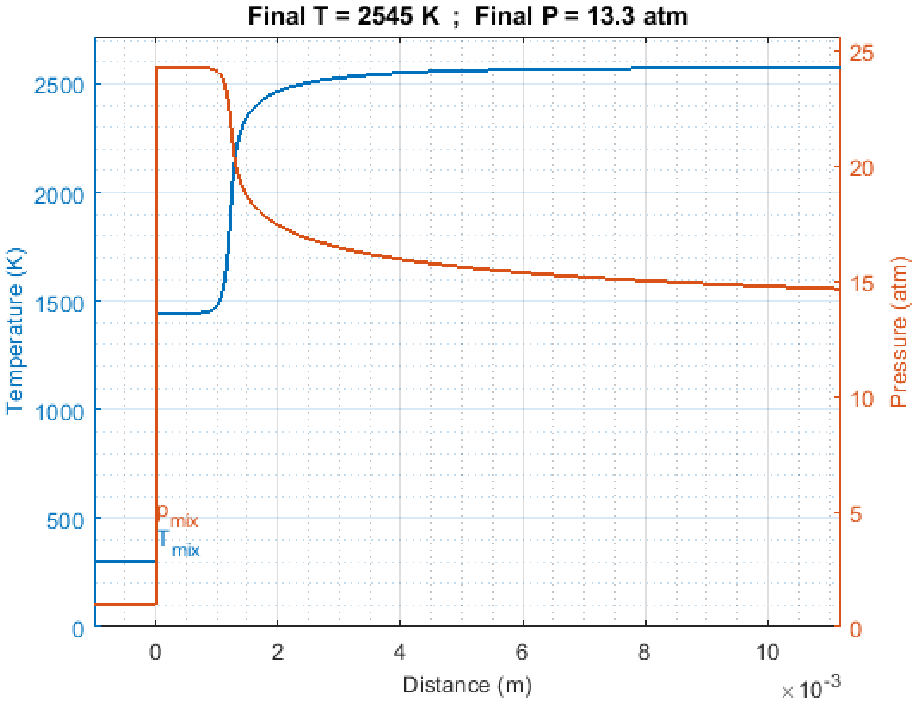

(b) *Upper limit* (90% of Hydrogen)

Figure 5.12: Hydrogen-Oxygen detonation structure at detonation limits

Like for deflagrations, even for detonations it is possible to define a lower and a upper *detonation limit* (LDL,UDL) as the minimum and the maximum fuel concentration outside of which detonation wave can not propagate. In general flammability limits are more extensive than detonation limits which represent a more limiting condition. However they were influenced by many factors whereby detonation limits can be different from mixture to mixture. The main paramaters which can alter the limits are initial conditions (temperature, pressure, equivalence ratio), geometry (confined or unconfined) and also the experimental apparatus [43]. For instance, detonation limits for an hydrogen-oxygen mixture at T=300 K and p=1 atm are about respectively equal to 15% and 90% [10].

From fig.5.12 it is possible to observe that the strongest detonation happens at stoichiometric composition. Infact pressure and temperature values are lower near the detonation limits. This happens because at stoichiometric compostion all the fuel reacts and the energy released is higher. Moreover in hydrogen-lean mixtures the induction zone length is very huge compared to stoichiometric condition. On the other hand, the greater is the hydrogen percentage in the mixture, the greater is the propagation velocity (tab. 5.2), since it is proportional to the reciprocal of the product molecular weight. Therefore for fuel-rich mixtures, the molecular weight is less and the propagation velocity is higher [23].

Table 5.2: C-J velocity comparison

COMPOSITION	C-J VELOCITY (m/s)
STOICH	2836
LDL	1415
UDL	3800

For fuel-air mixtures the denotation limits are reported in the next table (tab.5.3). Hydrogen-air detonation limits are narrower than both hydrogen-oxygen ones and hydrogen-air flammability limits. Instead, range of methane concentrations which permits detonation to propagate is taken from some experimental tests conducted at NIOSH Lake Lynn Laboratory [57].

Table 5.3: Fuel-Air detonation limits

FUEL	LDL	UDL
H_2	18	60
CH_4	~ 5.3	~ 15

As one expected final temperature and pressure are maximum near the stoichiometric composition, while they tend to decrease by approaching the detonation limits. Therefore stoichiometric is the most dangerous condition. Unlike hydrogen mixtures, methane-air system presents the maximum propagation speed at stoichiometric composition (fig.5.13).

Tab.5.4 summarizes the values of the different analyzed properties at detonation limits:

Table 5.4: Detonation characteristics at LDL and UDL

	H_2		CH_4	
	LDL	UDL	LDL	UDL
V_{CJ} (m/s)	1609	2300	1490	1790
T_{CJ} (K)	2194	1951	2004	2410
p_{CJ} (atm)	11.5	10.3	11.5	15.7

It is good to point out that detonation limits discussed in this section are evaluated using shock tube, so they could be quite different in the case of detonations in unconfined spaces.

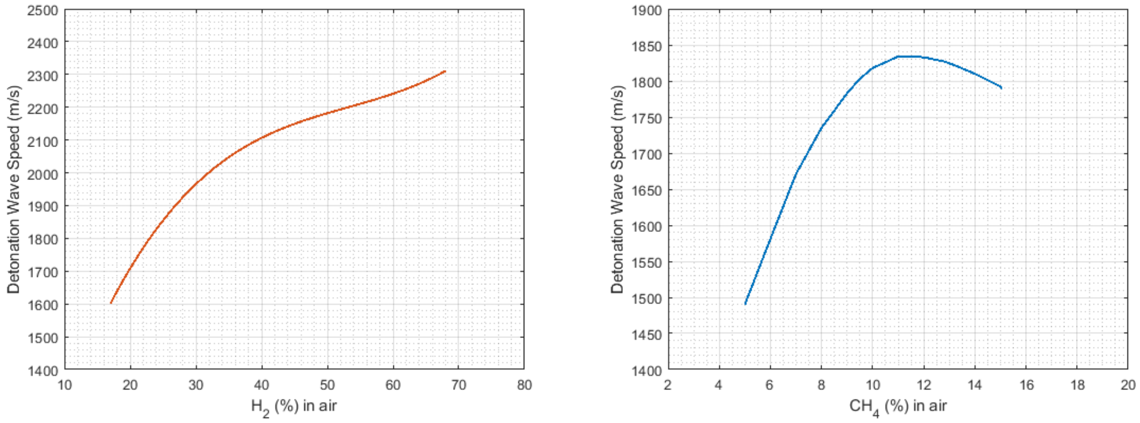

(a) V_{CJ} Hydrogen **(b)** V_{CJ} Methane

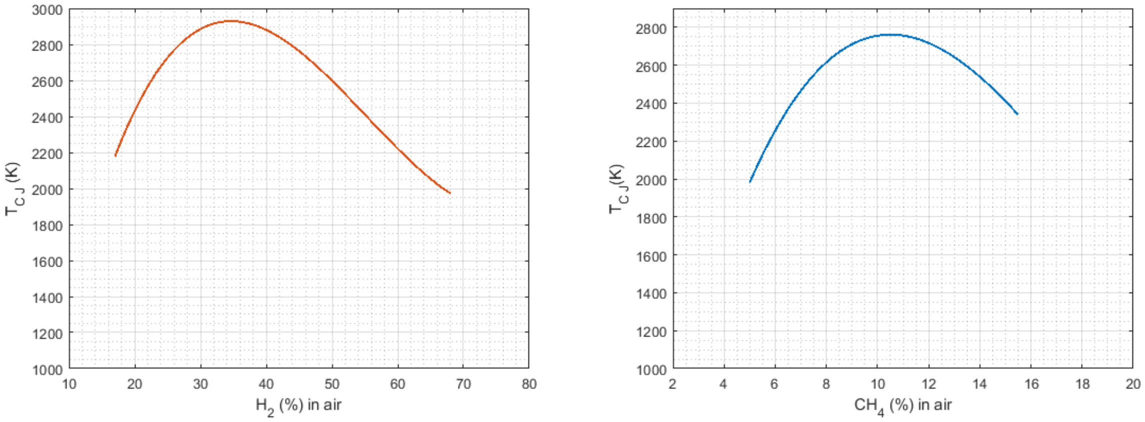

(c) T_{CJ} Hydrogen **(d)** T_{CJ} Methane

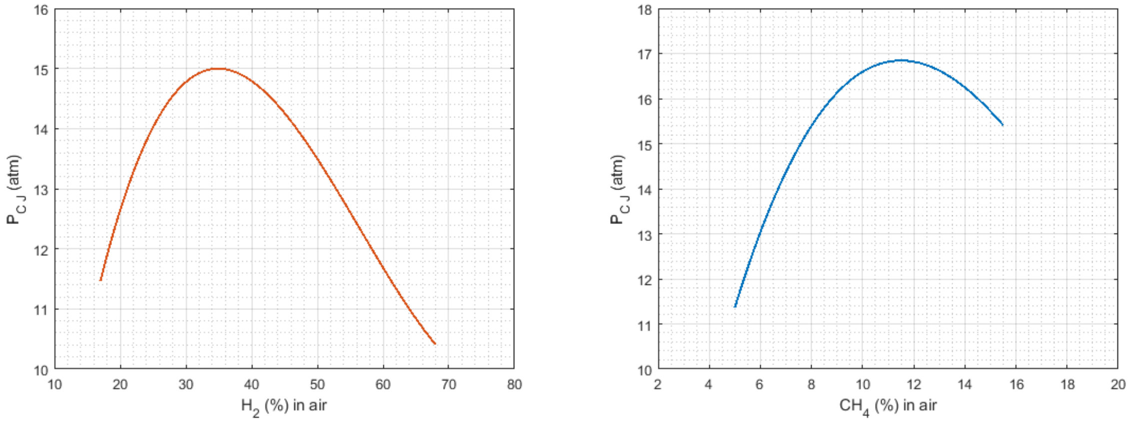

(e) p_{CJ} Hydrogen **(f)** p_{CJ} Methane

Figure 5.13: Effect of fuel concentration

5.4.2 Initial Temperature

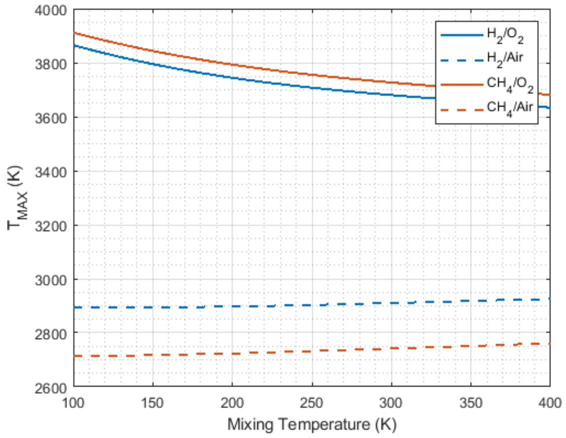

(a) T_{MAX}

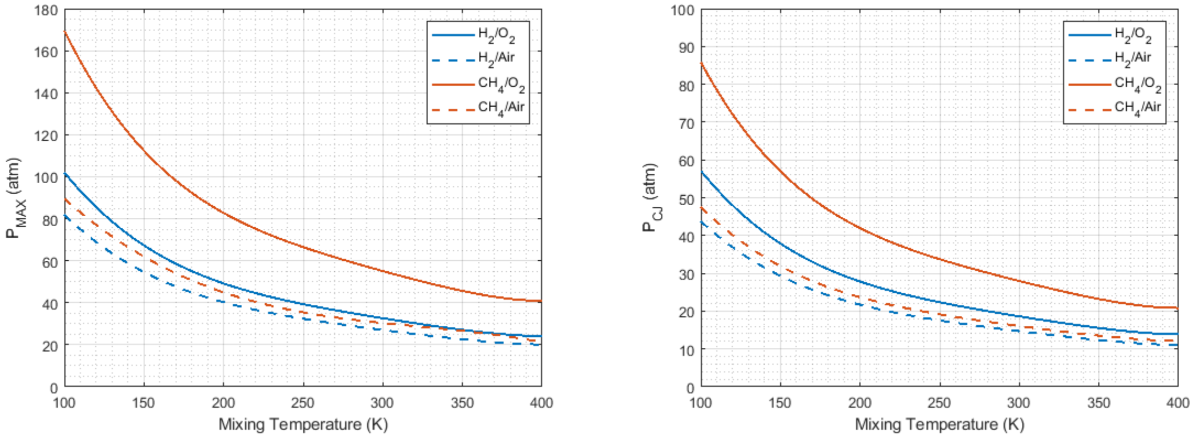

(b) p_{MAX} **(c)** p_{CJ}

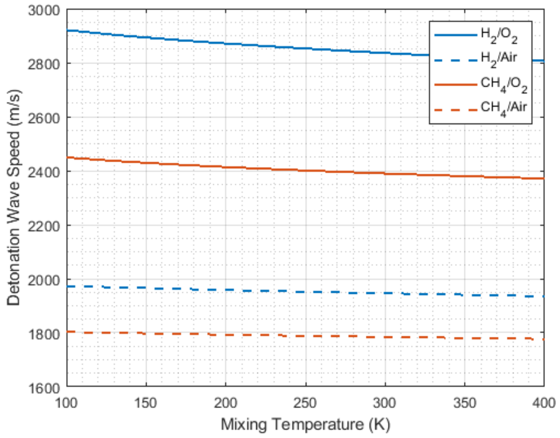

(d) V_{CJ}

Figure 5.14: Effect of initial temperature and composition

In fig.5.14 is illustrated the dependence of the detonation wave characteristics on the initial/mixing temperature. Analysis show that the maximum temperature, as well as post-shock and final temperature, mainly depends on composition while it is little affected by the initial temperature. Analougus speech for the C-J velocity. Instead, pressure strongly depends on the mixing temperature, so the curves for different composition are very close to each other.

Altough it may seems unusual that very low temperatures allow a detonation wave to propagate, the strongest blast happens for both hydrogen and methane system at cryogenic condition ($T \sim 100$ K) where the values of temperature and pressure are maximum. Despite of the greater energy needed to initiate the phenomenon (Mach number of the initial leading shock could be $>$7), maybe an important role is played by the density. At lower temperature the density is higher, so in the same volume there is a bigger concentration of molecules and the energy released per unit volume is greater.

Chapter 6

Overview on Liquid Cryogenic Propellant Hazards

In aerospace applications, hydrogen and methane are used prevalently in the liquid phase as propellants for space vehicles. Despite cryogenic temperatures are necessary to keep the propellants in a liquid state (tab.1.1), however they may originate explosions under certain conditions, above all after failures during the first phases of space vehicle launches. In addition, analysis of Sec.5.4.2 have shown that gaseous mixtures at initial cryogenic conditions, which can be originated by tank spill or ruptures, may produce the strongest detonations. For this reason, NASA have conducted many tests during the last 50 years in order to evaluate the risks and the explosion mechanisms of these liquid propellants.

6.1 LH2/LOx Experimental Tests

The development of space manned missions and the use of launch vehicle containing more and more propellant made a detailed study on liquid propellant blast hazards necessary. Actually, whereas the explosion hazards associated with liquid methane use are still under study, since it maybe will exploit in "future" missions, many tests and large-scale test programs have been carried out with LH2/LOx combinations. Therefore this section will focus mainly on experimental tests involving liquid Hydrogen and liquid Oxygen, and then a possible extension of the results to methane will be presented.

One of the most interesting and dangerous aspect about LH2/LOx propellant combination is related to their capability to self-ignition. Infact, preliminary investigations by *Gail et al.* have demonstrated that if liquid hydrogen and liquid oxygen fluxs come into contact, reactions may start without external heat source [21]. The same results were obtained through ”Dewar” tests, which were carried out to simulate the explosive hazards from a launch-vehicle failure.

In this case, both fuel and oxidizer were contained inside an alluminium pan: in the specific, glass dewars held liquid oxygen while liquid hydrogen filled the entire pan (fig.6.1). In the I phase of the program, pan was dropped on the ground resulting in a random shattering of the dewars, while in the II phase some detonating fuse were used to break the dewars. Some off-centered and localized explosion were obtained respectively in the first and second case. Anyway, tests showed that reactions started spontaneously and the explosive yield was proportional to the contact area between fuel and oxidant and to the mixing time between the rupture and the ignition: the greater are these factors, infact, the greater is the amount of mixed propellant [28].

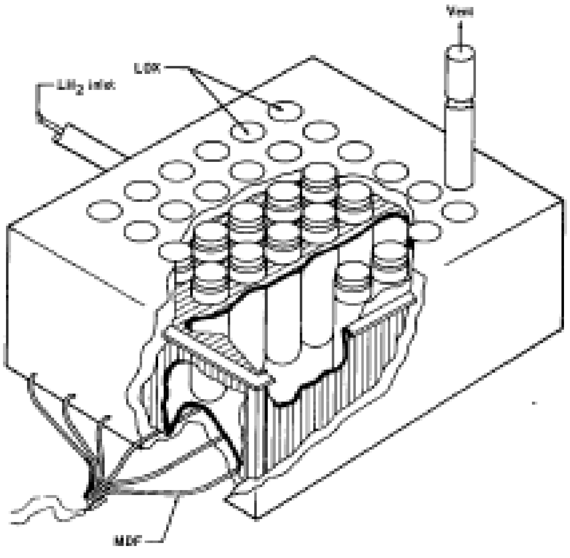

Figure 6.1: Dewar test device [28]

In conclusion both the previous investigations have shown that LH2/LOx quickly ignite spontaneously, but the cause for which this happens is unknown; moreover, the measured overpressures are lower than characteristic detonation ones. More accurate details can be found in Ref.[21, 28].

6.2 HOVI Tests

To better understand the mechanism of self-ignition and the explosion characteristics of LH2/LOx, NASA conducted a series of Hydrogen-Oxygen Vertical Impact Test (HOVI) in order to simulate the potential hazards connected with several tank rupture scenarios. Actually, these tests were performed after the *Challanger disaster* in 1986 in which an H2 gas leak through the O-ring results in the acceleration and subsequent impact of the LH2 tank with that of LOx, causing it to break [19]. Then the resulting mixture composed of GH2/GOx and LOx spontaneously ignited in the inter-tank zone where no apparent ignition sources were present and despite the temperatures were really low to maintain the propellant in the liquid phase. An other scenarios which can lead to an explosion could be the leak of liquid propellant from a tank and its splash on the ground or any other surface; even the failure of a vehicle stage with the consequent detachment and fall of the other stage tanks full of propellant, resulting in a violent impact on the ground and the release of their content, could be a possible damage situation [44].

In the HOVI tests, some tank configurations were used in order to simulate several failure scenarios (fig.6.2a). The various set-ups differ in the number of propellant tanks used and in the location of the rupture devices. In particular the different tests can be divided in two groups depending on the rupture device position: HOVI tests 13,14 (left image of fig.6.2a) belong to the first group, tests 2 and 5 (right picture of fig.6.2a) to the second group, while in 9 (first group) and 10 (second group) the double tank configuration is used (middle image of fig.6.2a) . Anyway, whatever the configuration is, the break of the tanks leads to the onset of an aerosol cloud consisting of GH2/GOx and liquid oxygen droplets (fig.6.2b), and its subsequent explosion although no trigger source is present nearby. The explosion happens on the ground or in the inter-tank space depending on whether the test belongs to the first or second group. For a detailed explanation about the tests and their development, the experimental set-up (including dimensions and materials of the tanks, amount of liquid propellant contained in the tanks and the escaped percentage etc.), see Ref.[44, 46].

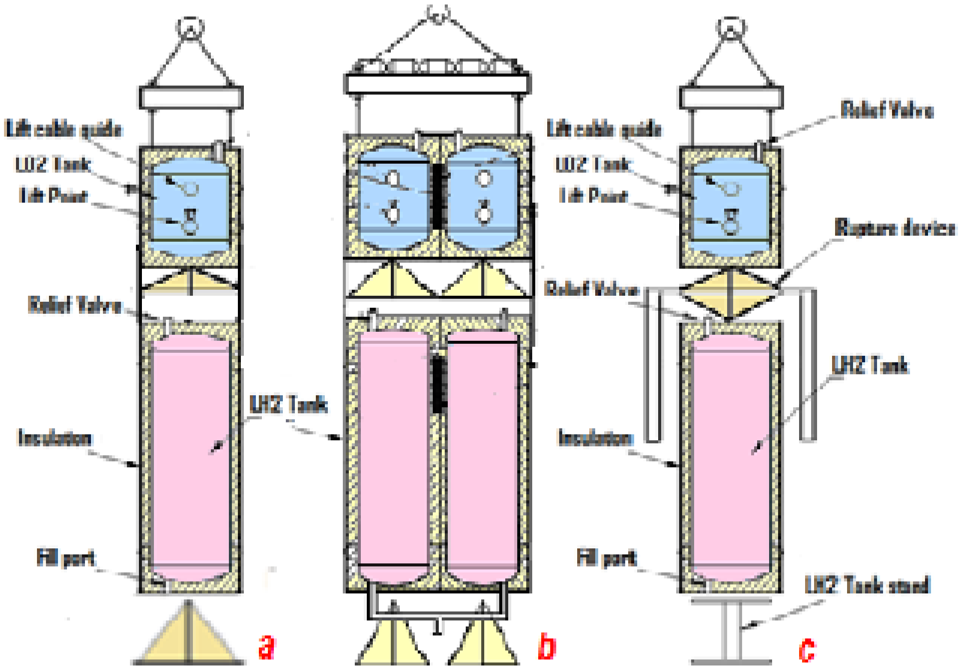

(a) Tank Configurations

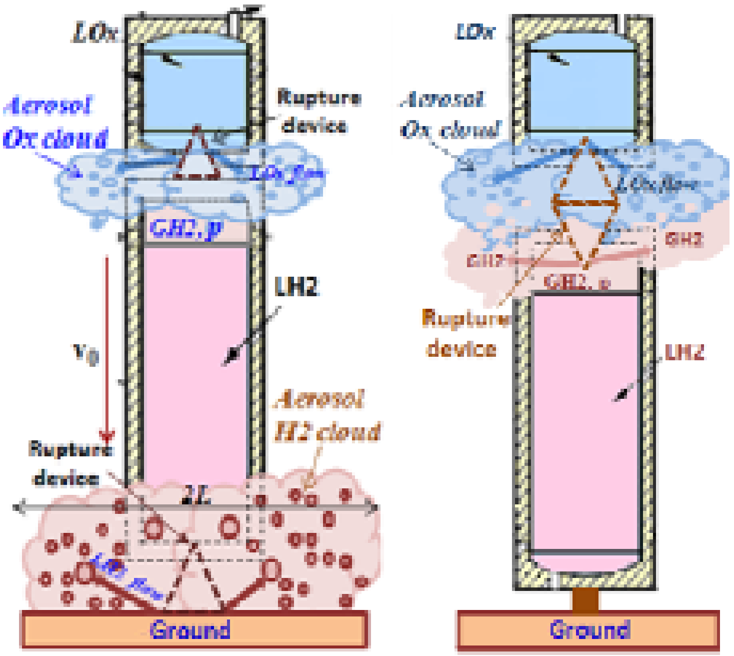

(b) Aerosol cloud onset

Figure 6.2: HOVI tests [44]

HOVI test results, taken from Ref.[46], are reported in tab.6.1. In particular, they can be compared with the characteristic values of deflagrations and detonations for gaseous mixtures, which have been discussed previously.

Table 6.1: HOVI test results and comparison

	Time delay (ms)	Maximum pressure (atm)	Pressure wave speed (m/s)
	HOVI tests (group)		
13 (1)	~ 90	$3.3 \div 4.2$	$\sim 740 \div 920$
14 (1)	~ 130	$3.4 \div 4.3$	$\sim 620 \div 925$
9 (1)	~ 200	$80 \div 110$	$\sim 2625 \div 2966$
2 (2)	~ 20	$3.2 \div 5.4$	~ 780
5 (2)	< 1	$2.5 \div 3$	660
10 (2)	< 1	$1.2 \div 1.4$	600
	Deflagration		
		~ 1	$\sim 40 \div 80$
	Detonation		
		~ 80	~ 2000

Deflagration and detonation characteristics in tab.6.1 are calculated at initial cryogenic conditions, p=1 atm and T=100 K. Deflagration pressure wave speed, related to a fixed observer, can be evaluated as $S_F = S_L \frac{T_{flame}}{T_{mix}}$ [46]. Considering $S_L = 1.5 \div 3$ m/s (fig.3.5), $T_{flame} =\sim 2500$ K (fig.2.5) and $T_{mix} = 100$ K, then $S_F =\sim 40 \div 80$ m/s. Pressure change across deflgration wave is negligible, as discussed in Sec.3.3.2, therefore maximum pressure is considered equal to the initial pressure. These values of pressure and velocity are quite similar to those obtained experimentally at standard condition [52].

Instead, the maximum pressure and wave speed, reported in the table, for a detonation in unconfined GH2/GOx/GN2, are taken from the analysis of Sec.5.4.2.

6.2.1 Comments on HOVI tests

Starting from the comparison shown in tab.6.1, several important considerations on the HOVI tests, the risks and the explosion mechanisms involving LH2/LOx can be made.

First of all, HOVI tests confirmed the tendency of LH2/LOx to self-ignite without external source. In particular, LH2 does not ignite alone, but explosive reactions take place in a very short time and only after the turbulent mixing with LOx [46]. The power of the explosion depends on the position at which aerosol cloud is formed after the rupture of the tanks. As one can see from fig.6.2b on the left side, related to the first group, the two clouds of hydrogen and oxygen are formed in separate zones. Therefore they need more time to come into contact forming a single one, which in addition occupies a larger area compared to the second group case (fig.6.2b right). This means that the time delay between tank failures and explosion is greater (thus the mixing is better) as well as the cloud size is larger, and for these reasons explosions in the first group tests are more powerful (greater values of pressure and velocity in tab.6.1).

In Sec.3.3 and in tab.5.1, the characteristics of deflagrations and detonations in gaseous hydrogen/oxygen mixtures at initial standard conditions have been discussed. It is possible to note that pressures and velocities from the HOVI tests are totally different compared to the typical values for deflagrations and detonations in gaseous mixtures, both at standard and cryogenic initial conditions. In fact, only in HOVI test 9 maximum pressure and propagation velocity are close to the values for a gaseous detonation (fig.5.14b and 5.14d), therefore just in this case a detonation occurs; in all the other situations, pressures and velocities are too high to consider the explosion as a simple deflagration, but they are too low for a detonation.

This means that the two-phase nature of the aerosol cloud (gaseous and liquid) plays a fundamental role and must be considered. Probably, the heat released by the initial ignition of GH2/GOx causes droplet evaporation and the subsequent increase of the amount of propellant available for reactions. This results in flame acceleration, formation of fast deflagration waves, and, maybe, only in HOVI 9, in a deflagration-to-detonation transition (DDT) [46]. In addition, it's more probable to have a DDT in unconfined aerosol mixtures, because liquid phase is more unstable than gaseous one, so in two-phase systems detonations can be started quite more easily, even with a small heat source (Sec.4.5).

6.2.2 Cavitation

In the prevoius discussions, it has been pointed out that liquid oxygen and hydrogen spill from a container can form an explosive aerosol cloud, even though no ignition source is available. The mechanism responsible for ignition of cryogenic H2/O2 mixtures has not been known yet. To explain this phenomenon of spontaneous ignition, recently *Osipov et al.* have proposed a mechanism involving cavitation of liquid oxygen [45].

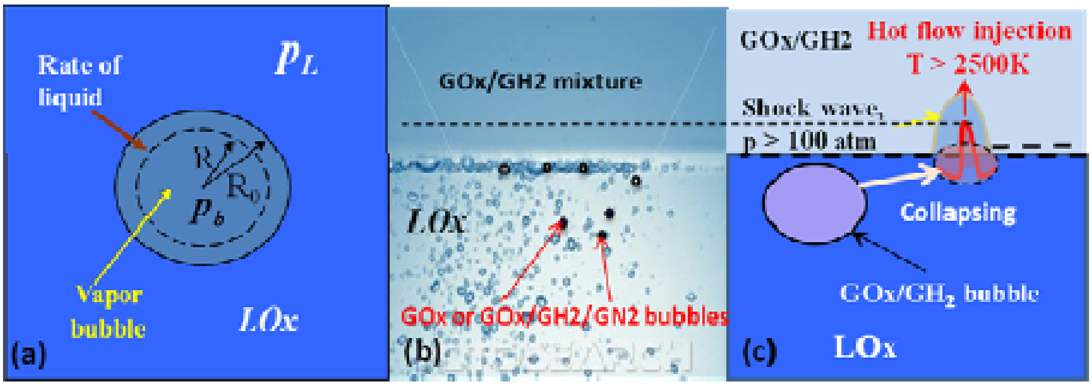

Figure 6.3: Cavitation-induced mechanism [44]

Cavitation consists in the growth and subsequent collapse of vapour bubble inside a liquid because of a sudden pressure jump. In fact, at constant temperature, if the liquid pressure locally falls below the vapour pressure, bubble starts growing and then, because of liquid inertial motion, they implodes [3]. For instance, the pressure jump required to initiate cavitation in the HOVI tests (Dewar tests) or during any launch failure, could be due to the turbulent mixing of the liquid oxygen stream with the GH2/GOx mixture, or even to a ”weak shock wave” forming after the impact of a liquid blob with a surface. Different scenarios, which can initiate the cavitation phenomenon, are discussed in [45].

However, the collapse of cavitation bubbles produces an abrupt increase of gas pressure and temperature inside the bubble, resulting in a strong shock wave which could propagate through the aerosol mixture, near the liquid oxygen interface, causing its explosion (fig.6.3).

The dynamic of a single bubble in a liquid is regulated by the *Rayleigh-Plesset equation* (eq.6.1). For an incompressible and viscous liquid, neglecting the surface tension, and in the assumption of spheric simmetry, the Rayleigh-Plesset equation is [3]:

$$\boxed{R\frac{d^2R}{dt^2}+\frac{3}{2}\left(\frac{dR}{dt}\right)^2+\frac{4\nu_L}{R}\frac{dR}{dt}=\frac{p_B(t)-p_L}{\rho_L}} \tag{6.1}$$

$R(t)$ is the bubble radius, ρ_L and ν_L are the liquid density and dynamic viscosity, $p_B(t)$ is the pressure inside the bubble and p_L is the liquid pressure far from the bubble. In this specific case, bubble can contain vapour oxygen and small quantities of gas H2, whose partial pressure is p_{g_0}, because some H2 molecules could become trapped inside liquid oxygen during the fall. Assuming that compression of gaseous hydrogen inside the bubble is an adiabatic process and neglecting thermal effects, p_b can be modeled as [3]:

$$p_B = p_{O_2} + p_{g_0}\cdot\left(\frac{R_0}{R}\right)^{3\gamma} \tag{6.2}$$

Here R_0 is an initial bubble radius and p_{O_2} is the saturation pressure of the oxygen vapour depending on the temperature at liquid-bubble interface.

Eq.6.1 has been resolved through Matlab routine ”ODE 15s” for some pressure differences Δp between liquid oxygen and bubble, several gaseous hydrogen partial pressures and an initial collapsing bubble radius of 2 mm. After the radius calculation, it’s possible to evaluate the pressure and temperature inside the bubble. For temperature it has been assumed an initial value of 90 K. Results are shown in fig.6.4a,6.4b,6.4c and tab.6.2.

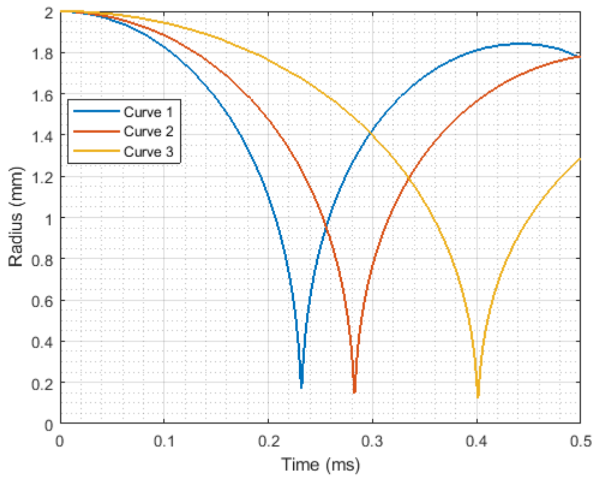

(a) Radius

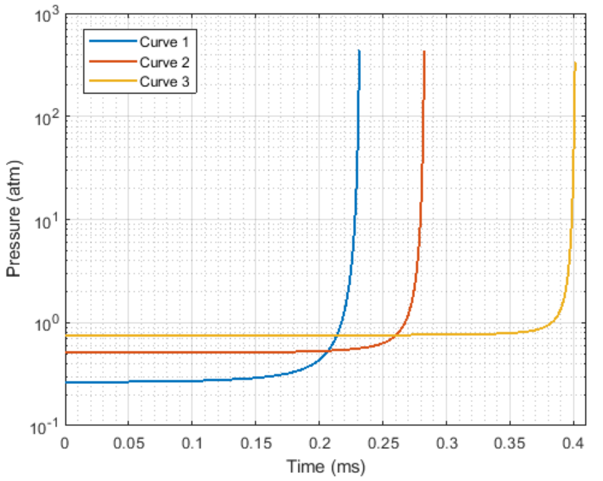

(b) Pressure

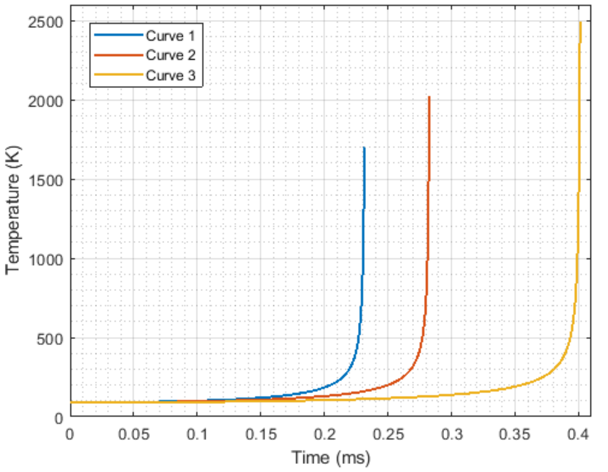

(c) Temperature

Figure 6.4: Bubble collapse

Table 6.2: Bubble collapse parameters

	Curve 1	Curve 2	Curve 3
Δp (atm)	0.75	0.5	0.25
p_{O_2} (atm)	0.25	0.5	0.75
p_{g_0} (atm)	0.015	0.008	0.003
R_{min} (mm)	0.173	0.149	0.125
t_{coll} (ms)	0.23	0.28	0.40
p_{max} (atm)	441	431	337
T_{max} (K)	1700	2040	2500

Results of tab.6.2 are in good agreement with those reported in Ref.[44]. As illustrated in the table, very high values of pressure and temperature (p>300 atm, T>1500 K) can be reached inside the bubble, even for small pressure jump (and so for weak initiating shock waves). Results are obtained neglecting combustion reactions which, clearly, occur inside the bubble because of the large pressures and temperatures. The injection of this hot and compressed products and/or the propagation of a strong shock wave, produced by the sudden expansion of the gases when bubbles implode, in the aerosol GH2/GOx/GN2 mixture, can easily ignite the cloud and generate the explosions observed in the HOVI tests [46].

6.3 Considerations on Liquid Methane

As seen in HOVI test section, the explosion mechanisms involving cryogenic liquid propellants are really complex and include a considerable number of puzzling parameters. Therefore it's very hard to figure out without appropriate experimental tests if previous results can be exdended to others propellant combinations like LCH4/LOx. Nevertheless some basic considerations can be made.

In the case of tank failures and propellant spill, impact of liquid blob on a surface might induce cavitation not only in LO2, like in LH2/LOx situation, but even in LCH4. Infact, methane has a higher boiling temperature, therefore it needs more time to evaporate, unlike hydrogen which passes to the vapour phase almost immediately after the tank rupture. Moreover, at the same temperature, the vapour pressure of liquid methane is lower than oxygen, thus cavitation requires a greater pressure jump to be initiated. Surely, the case of LCH4/LOx is more difficult to study and specific analysis are necessary to understand if cavitation occurs and what characteristics it has.

An other possible difference could be in the aerosol cloud formation and combustion, in which one of the key point is the fragmentation of the liquid into droplets. In the tests discussed above, aerosol mixture is formed by oxygen and hydrogen in gaseous and liquid droplets. The average radius of liquid droplets impinging on a smooth surface can be calculated with eq.6.3 [46, 2]:

$$r = 2.53 \cdot 10^5 d_h Re^{-1.28} We^{0.4} (\mu_L/\mu_{air})^{-1.16} \tag{6.3}$$

where Re and We are Reynolds and Weber number, respectively equal to: $Re = \frac{d_h v_L \rho^L}{\mu_L}$ and $We = \frac{d_h v_L^2 \rho^L}{\sigma_L}$. Instead, μ is the dynamic viscosity, d_h is the stream diameter, σ is the surface tension and v_L the liquid velocity.

Assuming $v_L = 30$ m/s and $d_h = 0.1$ m (Sec.II of [46]), $\mu_{air} = 1.63 \cdot 10^{-5}$ Pa·s, $\mu_{H_2} = 1.32 \cdot 10^{-5}$ Pa·s, $\mu_{O_2} = 1.96 \cdot 10^{-5}$ Pa·s, $\sigma_{H_2} = 1.65 \cdot 10^{-3}$ N/m, $\sigma_{O_2} = 7.3 \cdot 10^{-3}$ N/m, from eq.6.3 it results that hydrogen and oxygen droplet radius are ~ 8 mm and ~ 0.5 mm. For methane, instead, using the same equation, it would be of the order of ~ 0.05 mm, thus methane droplets would be much smaller than hydrogen and oxygen ones. This means that droplet evaporation would not increase the combustible gas density significantly as in LH2/LOx case, therefore it is more difficult for flame acceleration and DDT to take place. Moreover, also the heat transfer mechanism from the hot products to the droplet is less efficient because of the lower thermal conductivity (fig.1.3).

In addition, some tests performed on methane-air and methane-oxygen-nytrogen mixtures during 1970s, in order to study possible explosions which could rise from release of liquid natural gas, have shown that methane unconfined detonations are unlikely [57, 29]. For all these reasons, at the current knowledge it seems that LH2/LOx explosion scenarios and self-ignition mechanisms talked about in this chapter cannot be referred to liquid methane too, but more detailed tests and analysis are necessary to better understand explosive properties of methane mixtures.

Chapter 7

Conclusions

Explosion risks and safety related to the use of flammable substances are and always will be a current issue. Many studies, data, experimental results on hydrogen and methane explosions are sparse in literature. The purpose of this work is to collect and put togheter the most important information found in several documents, in order to provide a possible help for future analysis.

What is clear from this work is that explosions are very complex phenomena which depend on a huge number of parameters. Therefore, when speaking of the possible methane and hydrogen hazards, it would not be corrected to generalize, since even a small change of some conditions may lead to different scenarios.

In general chemical explosions are regulated by the elementary reactions reported in Ch.2 and especially by the formation of reactive and unstable radical species. Therefore, for a mixture to become explosive, temperature and pressure have to maintain a certain number of branching reactions in which the produced radicals are more than the starting ones. However, from an initial analysis of this work, hydrogen seems to be more dangerous and to have greater tendency in forming explosive mixtures than methane. This conclusion comes from a whole series of observations and considerations.

First of all hydrogen is more reactive than methane, because the covalent bond between carbon and hydrogen atoms in the methane molecule needs more energy to be broken and start the oxidation process; in addition, it allows flames to propagate for a wider range of fuel concentrations: (LFL,UFL)=(5 , 95) % and (5 , 75) % for hydrogen respectively in oxygen and air, while (LFL,UFL)=(5 , 61) % and (5 , 15) % for methane.

Comparing the mechanisms and the typical characteristics of deflagration and detonation phenomena, it is evident that the worst explosion scenario is represented by detonations in fuel-oxygen systems. In fact, analysis of Ch.5 show that, at stoichiometric composition and initial standard conditions, the temperature and pressure jump through the wave is equal to $\Delta T =\sim 3000$ K and $\Delta p =\sim 14 \div 18$ atm. On the other side, this means that detonations need much more energy to be initiated and, therefore, the leading shock wave must propagate to a Mach number at least >4. These values are even greater in the case of initial cryogenic conditions in which, despite the initial very low temperatures (~ 100 K), the strongest blast is formed. Maybe it is due to the higher value of density: this means that in the same volume there is a bigger concentration of molecules and the energy released per unit volume is bigger.

Anyway, detonation can be formed by direct initiation or deflagration-to-detonation transition. Because of the huge amount of energy required by the first mechanism, the most probable initiation mechanism in accidental explosions is represented by DDT. It consists in a flame acceleration process due to turbolence and instabilities, until the conditions necessary to rise a detonation are reached. Therefore it is more likely to happen in confined space and in presence of obstacle where their interaction with the pressure waves increases turbolence.

In the case of two-phase mixtures (spray or aerosol) explosion features are different compared to gaseous state. The precence of liquid droplets seems to help flame acceleration because of droplet evaporation and subsequent increase of propellant mass available for the combustion. However, once again, DDT may happen more easily in hydrogen mixtures where the propagation velocity of deflagration waves is higher.

Finally, detailed tests and analysis would be needed to comprehend if LCH4/LOx had the same capability of LH2/LOx to self-ignite and generate explosions without external heat source, as shown in the HOVI tests. In fact, at the current knowledge unconfined detonations of gaseous/liquid methane are unlikely.

Bibliography

[1] *Adiabatic Flame Temperature.* URL: `http://web.mit.edu/16.unified/www/FALL/thermodynamics/notes/node111.html`.

[2] M Ahmed, N Ashgriz, and HN Tran. "Influence of breakup regimes on the droplet size produced by splash-plate nozzles". In: *AIAA journal* 47.3 (2009), pp. 516–522.

[3] Christopher E Brennen. *Cavitation and bubble dynamics.* Cambridge University Press, 2013.

[4] S Brown and JE Shepherd. "Numerical Solution Methods for Control Volume Explosions and ZND Structure". In: *GALCIT Report, July* (2005).

[5] S Brown and JE Shepherd. *Numerical solution methods for shock and detonation jump conditions. GALCIT Report FM 2006.006.* 2004.

[6] S Browne, J Ziegler, and JE Shepherd. "Shock and Detonation Toolbox". In: *GALCIT-Explosion Dynamics Laboratory, Pasadena, CA* (2008).

[7] DC Bull, MA McLeod, and GA Mizner. "Detonation of unconfined fuel aerosols". In: *Progress in Astronautics and Aeronautics* 75 (1981), pp. 48–60.

[8] A Cavaliere. *Lezioni di Combustione.* 2001.

[9] David Leonard Chapman. "VI. On the rate of explosion in gases". In: *The London, Edinburgh, and Dublin Philosophical Magazine and Journal of Science* 47.284 (1899), pp. 90–104.

[10] N. Cohen. *Flammability and Explosion Limits of H2 and H2/CO: A Literature Review.* Report. Space and Environment Center Technology Operations, 1992.

[11] *Combustion on Wikipedia.* 2018. URL: `https://en.wikipedia.org/wiki/Combustion`.

[12] *Combustion-NASA.* 2015. URL: `https://www.grc.nasa.gov/WWW/k-12/airplane/combst1.html`.

[13] Daniel A Crowl and Joseph F Louvar. *Chemical process safety: fundamentals with applications.* Pearson Education, 2001.

[14] EK Dabora, KW Ragland, and JA Nicholls. "Drop-size effects in spray detonations". In: *Symposium (International) on Combustion.* Vol. 12. 1. Elsevier. 1969, pp. 19–26.

[15] *Detonation Front Structure.* URL: `https://en.wikibooks.org/wiki/Engineering_Acoustics/Detonation`.

[16] TD Donakowski. "Is liquid hydrogen safer than liquid methane?" In: *Fire Technology* 17.3 (1981), pp. 183–188.

[17] Werner Döring. "On detonation processes in gases". In: *Ann. Phys* 43.421-436 (1943), p. 9.

[18] SB Dorofeev et al. "Deflagration to detonation transition in large confined volume of lean hydrogen-air mixtures". In: *Combustion and flame* 104.1-2 (1996), pp. 95–110.

[19] R Feynman. "Report of the presidential commission on the space shuttle Challenger accident". In: *Appendix F* (1986).

[20] Abdelkader Frendi and Merwin Sibulkin. "Dependence of minimum ignition energy on ignition parameters". In: *Combustion science and technology* 73.1-3 (1990), pp. 395–413.

[21] JB Gayle et al. "Preliminary investigation of blast hazards of RP-I/LOX and LH2/LOX propellant combinations". In: *NASA Technical Memorandum X-53240* (1965).

[22] GJ Gibbs and HF Calcote. "Effect of molecular structure on burning velocity." In: *Journal of chemical and engineering data* 4.3 (1959), pp. 226–237.

[23] I. Glassman and R. A. Yetter. *Combustion, Fourth Edition.* Milano: Elsevier, 2008.

[24] David G Goodwin, Harry K Moffat, and Raymond L Speth. “Cantera: An object-oriented software toolkit for chemical kinetics, thermodynamics, and transport processes”. In: *Caltech, Pasadena, CA* (2009).

[25] DG Goodwin. “An open-source, extensible software suite for CVD process simulation”. In: *Chemical vapor deposition XVI and EUROCVD* 14.40 (2003), pp. 2003–08.

[26] M Groethe et al. “Large-scale hydrogen deflagrations and detonations”. In: *International Journal of Hydrogen Energy* 32.13 (2007), pp. 2125–2133.

[27] Ali Heidari and Jennifer X Wen. “Numerical simulation of flame acceleration and deflagration to detonation transition in hydrogen-air mixture”. In: *International Journal of Hydrogen Energy* 39.36 (2014), pp. 21317–21327.

[28] Richard W High. “Some liquid oxygen/liquid hydrogen explosive effects in controlled failure-mode tests”. In: (1969).

[29] Mike Hightower et al. *Guidance on risk analysis and safety implications of a large liquefied natural gas (LNG) spill over water.* Tech. rep. SANDIA NATIONAL LABS ALBUQUERQUE NM, 2004.

[30] Emile Jouguet. “Sur la propagation des réactions chimiques dans les gaz”. In: *J. Maths. Pure Appl.* 7 (1905), p. 347.

[31] Michael Kaneshige and Joseph E Shepherd. “Detonation database”. In: (1997).

[32] Robert J Kee, Fran M Rupley, and James A Miller. *Chemkin-II: A Fortran chemical kinetics package for the analysis of gas-phase chemical kinetics.* Tech. rep. Sandia National Labs., Livermore, CA (USA), 1989.

[33] DA Kessler, VN Gamezo, and ES Oran. “Simulations of flame acceleration and deflagration-to-detonation transitions in methane–air systems”. In: *Combustion and Flame* 157.11 (2010), pp. 2063–2077.

[34] Joseph M Kuchta. “Investigation of fire and explosion accidents in the chemical, mining, and fuel-related industries”. In: *Bull./US. Dep. of the interior Bureau of mines* (1985).

[35] Chung K Law. *Combustion physics.* Cambridge university press, 2010.

[36] John H. S. Lee. *The Detonation Phenomenon.* Cambridge University Press, 2008.

[37] John HS Lee. "Dynamic parameters of gaseous detonations". In: *Annual review of fluid mechanics* 16.1 (1984), pp. 311–336.

[38] John HS Lee. "Initiation of gaseous detonation". In: *Annual Review of Physical Chemistry* 28.1 (1977), pp. 75–104.

[39] Bernard Levis and Guenther Elbe. *Combustion Flames Explosions Gases.* Academic Press, 1961.

[40] MA Liberman et al. "Deflagration-to-detonation transition in highly reactive combustible mixtures". In: *Acta Astronautica* 67.7-8 (2010), pp. 688–701.

[41] Juan Ali Medina Mendez. *Application of LEM/ODT for the Evaluation of n-Heptane Premixed Turbulent Combustion.* Aug. 2016.

[42] Tetsu Nakamura. "Computational Analysis of Zel'dovich-von Neumann-Doering (ZND) Detonation". PhD thesis. Texas A & M University, 2010.

[43] Michael Arthur Nettleton. *Gaseous detonations: their nature, effects and control.* Springer Science & Business Media, 2012.

[44] Viatcheslav Osipov et al. "Hazards Induced by Breach of Liquid Rocket Fuel Tanks: Conditions and Risks of Cryogenic Liquid Hydrogen-Oxygen Mixture Explosions". In: *arXiv preprint arXiv:1012.5135* (2010).

[45] VV Osipov et al. "Cavitation-induced ignition of cryogenic hydrogen-oxygen fluids". In: *Applied Physics Letters* 98.13 (2011), p. 134102.

[46] V. Osipov et al. "Explosion Hazard from a Propellant-Tank Breach in Liquid Hydrogen-Oxygen Rockets". In: *JOURNAL OF SPACECRAFT AND ROCKETS* (2013).

[47] JE Shepherd. *Chemical kinetics of hydrogen-air-diluent detonations.[Kinetic models to predict detonation cell size].* Tech. rep. Sandia National Labs., Albuquerque, NM (USA), 1985.

[48] JE Shepherd and JHS Lee. “Major research topics in combustion”. In: *eds. MY Hussaini, A. Kumar, and RG Voigt, Springer, New York* (1992), pp. 439–490.

[49] Joseph E Shepherd and John HS Lee. “On the transition from deflagration to detonation”. In: *Major research topics in combustion.* Springer, 1992, pp. 439–487.

[50] J Shepherd et al. “Detonations in H2–N2O–CH4–NH3–O2–N2 mixtures, Explosion Dynamics Laboratory Report FM97-3”. In: *Graduate Aeronautical Laboratories, California Institute of Technology* (1997).

[51] Gregory P Smith et al. *GRImech 3.0 reaction mechanism, Berkeley.* 2012.

[52] S. Tretsiakova-McNally. *Lecture. Dealing with Hydrogen Explosions.* URL: `http://www.hyresponse.eu/files/Lectures/Dealing_with_hydrogen_explosions_notes.pdf`.

[53] John Von Neuman. *Theory of detonation waves.* Tech. rep. INSTITUTE FOR ADVANCED STUDY PRINCETON NJ, 1942.

[54] I Zel’dovich, S M Kogargo, and N N Semonov. “An Experimental Investigation of Sperifical Detonation of gas”. In: *Sov. Phys.-Tech.Phys* 1 (1956), pp. 1689–1713.

[55] Ya Be Zeldovich and GI Barenblatt. “Theory of flame propagation”. In: *Combustion and Flame* 3 (1959), pp. 61–74.

[56] Yakov Borissovich Zeldovich. “On the theory of the propagation of detonation in gaseous systems”. In: (1950).

[57] RK Zipf Jr et al. “Methane–air detonation experiments at NIOSH Lake Lynn Laboratory”. In: *Journal of Loss Prevention in the Process Industries* 26.2 (2013), pp. 295–301.

[58] Isaac A Zlochower and Gregory M Green. “The limiting oxygen concentration and flammability limits of gases and gas mixtures”. In: *Journal of loss prevention in the process industries* 22.4 (2009), pp. 499–505.

Ringraziamenti

Ringrazio il Prof. Pastrone e il Prof. Haidn per la disponibilità mostrata e per avermi concesso la possibilità di poter svolgere il mio lavoro di tesi all'estero.
Ringrazio i miei amici di Avellino, tutti gli amici conosciuti in questa esperienza torinese, la lunga lista di inquilini di VIA PEROSA e in particolar modo Aurelio, Raff, Michele, Lorenzo e Guasti con cui ho condiviso gioie e sopratutto ansie in questi 3 anni.
Ringrazio Alessia, i miei zii, cugini e nonni per il loro continuo sostegno e incoraggiamento.
Ringrazio mamma e papà per avermi sempre sostenuto moralmente ed economicamente e per aver sempre creduto in me. Questo traguardo è anche e sopratutto merito dei vostri sacrifici senza i quali tutto quello che ho fatto non sarebbe stato possibile.
Ringrazio Maria per aver accettato le mie scelte, per la pazienza, l'amore dimostratomi in questi anni e per essermi stata vicina nei momenti difficili. Grazie per avermi amato e sostenuto durante tutta questa esperienza, sei la migliore!
Infine, vorrei rivolgere un pensiero particolare a nonno Mario. Anche se non sei qui, sicuramente starai festeggiando insieme a noi questo giorno.